THE DEVELOPMENT OF BIODEGRADABLE METALLIC SCREWS AND SUTURE ANCHORS FOR SOFT TISSUE FIXATION IN ORTHOPAEDIC SURGERY

by

Kwang Eun Kim

Bachelor of Science, University of Washington, 2008

Submitted to the Graduate Faculty of
Swanson School of Engineering in partial fulfillment
of the requirements for the degree of
Doctor of Philosophy

University of Pittsburgh

2014

UNIVERSITY OF PITTSBURGH

SWANSON SCHOOL OF ENGINEERING

This dissertation was presented

by

Kwang Eun Kim

It was defended on

March 19, 2014

and approved by

David A. Vorp, Ph.D., William Kepler Whiteford Professor,

Department of Bioengineering

Prashant Kumta, Ph.D., Edward R. Weidlein Chair Professor,

Department of Bioengineering

Patrick J. McMahon, M.D., Adjunct Associate Professor,

Department of Bioengineering

Matthew B.A. McCullough, Ph.D., Assistant Professor, Department of Chemical, Biological, and Bioengineering, North Carolina Agricultural and Technical State University

Dissertation Director: Savio L-Y. Woo, Ph.D., D.Sc., D.Eng., Distinguished University Professor,

Department of Bioengineering

THE DEVELOPMENT OF BIODEGRADABLE METALLIC SCREWS AND SUTURE ANCHORS FOR SOFT TISSUE FIXATION IN ORTHOPAEDIC SURGERY

Kwang Eun Kim, PhD

University of Pittsburgh, 2014

Surgical treatment for injuries to soft connective tissues are estimated at about 800,000 cases each year in the US. For these surgical procedures, interference screws or suture anchors are needed. Currently, materials used for the devices are non-degradable metals or bioresorbable polymers. However, these materials do lead to complications. Metallic materials suffer from difficulties encountered during revision surgery and interference with magnetic resonance imaging; whereas, polymeric materials lead to device fracture during implantation, inconsistent degradation rates, and poor osteointegration.

The overall goal of this dissertation was to explore the use of Mg-based materials as an alternative to the existing materials. Specifically, the studies focused on Mg-based interference screws for ACL reconstruction and suture anchors for rotator cuff repair. First, a Mg-based interference screw was designed and optimized through in-vitro testing and finite element analysis (FEA). At time zero, ACL reconstruction with Mg-based interference screws was found to restore initial joint stability as well as the in-situ load in the ACL close to the levels of the intact. Also, structural properties of the femur-graft-tibia complex (FGTC) with a Mg-based interference screw were comparable as those with a titanium control. In a follow-up study, joint stability and graft function after 12 weeks of healing were found to be comparable to past studies of ACL reconstruction in a goat model using the robotic/UFS testing system. The stiffness and

ultimate load of the FGTC at 12 weeks were comparable to those at time zero. These results indicate that Mg-based interference screws allow for proper healing of the graft.

Similarly, a Mg-based suture anchor was also designed and developed. Using FEA, the thread depth and pitch of the anchor could be optimized. It was then demonstrated that Mg-based suture anchors could achieve superior fixation over commercially available polymer suture anchors as it could provide a higher stiffness and ultimate load.

In summary, the potential of Mg-based alloys for fixation of soft tissues to bone has been clearly demonstrated. We hope that the current findings would help the development of a novel class of biodegradable metallic implants that would ultimately help patients with improved outcomes.

TABLE OF CONTENTS

LIST OF TABLES

LIST OF FIGURES

1.0 MOTIVATION

Injuries to soft connective tissues in the musculoskeletal system, such as ligaments and tendons, are on the rise as participation in sports activities increase and the aging population grows. All soft tissue injuries combined, the total can be estimated to be more than 800,000 cases per year in the US (AAOS, 2008). To restore the stability and function of joints with soft tissue injuries, surgical treatment of the injured tissues is often required.

In the lower extremity, anterior cruciate ligament (ACL) is a good example as it is one of the most injured knee ligaments with more than 100,000 injuries each year in the US (Beaty, 1999). Two thirds of these cases will require either immediate or delayed surgical reconstruction to restore joint stability. With the cost per surgery (Cole et al., 2005), it is costing the society estimated $1 billion each year. For ACL reconstruction, soft tissue autografts or allografts are used as a replacement of the torn ACL (Aglietti et al., 1994; Nakamura et al., 2002; Spindler et al., 2004). These replacement grafts need to be securely fixed in bone tunnels. Among various fixation devices, interference screws are the most popular (Brand et al., 2000; Kurosaka et al., 1987) as they can fix the graft the closest to the joint space, reducing graft motion, which is thought to cause tunnel widening (Hoher et al., 1999).

In the upper extremity, rotator cuff tears are quite common with 8-26% of the population having a full-thickness tear (Cotton and Rideout, 1964) and 13-37% having a partial thickness tear (Breazeale and Craig, 1997; Fukuda, 2000; Fukuda et al., 1994). More than 300,000 surgeries are performed each year to repair torn rotator cuffs (Colvin et al., 2012). For rotator

cuff repair, suture anchors (screws with an eyelet to hold one or multiple sutures) are used to reattach the torn end of rotator cuff on the humeral head (Barber et al., 2008; Ozbaydar et al., 2007). Interference screws and suture anchors are also frequently used for other soft connective tissues including acetabular labrum (Philippon et al., 2007), patellar tendon (Capiola and Re, 2007), medial patellofemoral ligament (Kumahashi et al., 2012), and so on.

Soft-tissue fixation devices are either made of non-degradable metallic materials or bioresorbable polymers (Laxdal et al., 2006; Ozbaydar et al., 2007; Suchenski et al., 2010b). Metallic materials possess excellent mechanical properties (Li et al., 2010) and have demonstrated acceptable biocompatibility and osteointegration (Brand et al., 2005). However, their permanency complicates already challenging revision surgeries (Shen et al., 2010) and interfere with MRI making post-operative care difficult (Bowers et al., 2008; Shellock et al., 1992). Bioresorbable polymers have been designed to overcome these shortcomings as they are biodegradable and do not interfere with MRI (Ernstberger et al., 2010). In reality, polymer materials have unpredictable degradation rates ranging from less than 1 year up to 4 years (Stahelin et al., 1997; Walton and Cotton, 2007), cause inflammatory responses (Kwak et al., 2008; Macdonald and Arneja, 2003), leads to poor osteointegration (Moisala et al., 2008; Walton and Cotton, 2007), and frequently break during implantation (Smith et al., 2003). Hence, an alternative that overcomes these complications is desired.

Magnesium and its alloys (Mg-based materials) are rapidly gaining attention as a novel degradable material for orthopaedic applications (Hort et al., 2010; Staiger et al., 2006). These materials are bioresorbable and their degradation rates can be controlled through alloying and surface treatment without affecting their initial mechanical properties (Liao et al., 2013; Zberg et al., 2009). They also possess superior mechanical properties in terms of tensile strength, modulus,

and ductility compared to polymers (Gay et al., 2009). Further, Mg-based materials have been shown to be biocompatible and even osteoinductive in *in vivo* studies (Witte et al., 2005; Zhang et al., 2009). Minimal interference with MRI by Mg-based materials is also beneficial for post-operative care (Ernstberger et al., 2010). These advantageous properties of Mg-based materials make this an ideal alternative to the existing materials for soft-tissue fixation devices. ***Therefore, the overall goal of this dissertation was to develop Mg-based interference screws for ACL reconstruction and suture anchors for rotator cuff repair and to demonstrate feasibility of Mg-based materials for soft-tissue fixation in terms of biocompatibility and biomechanical performance.***

2.0 BACKGROUND

2.1 BIOLOGY AND BIOMECHANICS OF LIGAMENTS AND TENDONS

Ligaments and tendons are soft connective tissues that specialize in transmitting tensile loads. A ligament connects between two bones while a tendon connects a muscle to a bone. They are made of parallel collagen fibers that are packed together such that they can effectively transmit loads and provide motion and stability to joints.

2.1.1 Biochemical Composition and Histological Structure

Ligaments and tendons consist of various biochemical components that are intricately arranged to perform their functions effectively. The most abundant biochemical component in these tissues is water with its contribution reaching up to 70% of total weight. From dry weight, collagen type-I, the most abundant solid component, makes up roughly 70%. This subtype of collagen cross-links with one another to form larger structural units (Tanzer and Waite, 1982). Cross-linking is also essential for stability of the collagen fibers. Collagen type-V plays a important role as a regulator of this cross-linking as it was shown that high levels of this subtype were correlated with small diameters of collagen fibrils (Linsenmayer et al., 1993). Collagen type-XII is essential to smooth sliding of collagen fibers to reduce unnecessary energy loss (Niyibizi et al., 1995). Collagen type-XIV is concentrated at the soft-tissue-to-bone junction (Niyibizi et al., 1995). There are many other subtypes of collagen that serve essential functions.

Elastin, although only in few percents of dry weight of ligaments and tendons, works to restore the original length of the tissue after stretching. Proteoglycans are another class of molecules that make up a small percentage. These molecules are essential to regulation of water content within the extracellular matrix by holding positive charges to attract water and other ionic molecules. This is important for lubrication and gliding of collagen fibers that are essential to proper functioning.

Ligaments and tendons have a hierarchical organization from the smallest unit of fibrils to fibers, subfascicular units, fasciculi, and the tissue in the order of complexity. The tissue is often surrounded by a loose connective tissue, periligament and paratenon, which protects the ligament from abrasion and supports neurovasculature (Chowdhury et al., 1991). Ligaments and tendons are inserted to the bone through two distinct ways: direct and indirect insertions. Direct insertions have four distinct phases in the transition from the soft tissue to the bone: soft tissue, fibrocarticlage, mineralized fibrocartilage, and bone (Cooper and Misol, 1970; Woo et al., 1987a). The transition zone is generally less than 1 mm in length. Direct insertions are usually found those located before the epiphyseal plate. Indirect insertions are more complex and involve two distinct fibers, superficial and deep (or Sharpey) fibers. The superficial fibers are attached to the periosteum while the deep fibers are inserted in the bone (Cooper and Misol, 1970). Indirect insertions are located past the epiphyseal plate. Either direct or indirect, ligament and tendon insertions are constructed to minimize stress concentration and effectively transmit loads between a soft tissue to a bone.

2.1.2 Tensile Properties of Ligaments and Tendons

As the primary purpose of ligaments and tendons is transmitting tensile loads, it is logical to study their mechanical behavior in response to such loads. The most effective way to characterize ligaments and tendons mechanically is performing a uniaxial tensile test where a tissue specimen is loaded in tension in a single axis. From this we can obtain structural properties and mechanical properties.

2.1.2.1 Structural Properties of Bone-Soft Tissue-Bone Complex

An isolated soft tissue is difficult to test by itself due to limitations in size and difficulties in clamping; hence, ligaments and tendons are often tested with the bones attached (bone-soft tissue-bone complex). This makes it easier to clamp the specimen to a materials testing machine and allows for preservation of the tissue as much as possible. On a materials testing machine, the specimen is subjected to a load-to-failure test where it is elongated at a prescribed rate until failure occurs within the specimen. From this test, a load-elongation curve is obtained, which is usually non-linear (see **Figure A.1**). The curve has a gradual slope (low stiffness) in low elongations, which is called a toe-region. In this region, collagen fibers are recruited gradually, and the collagen fibers are still crimped (wavy), lowering the stiffness. As the tissue gets elongated more, more fibers are recruited and the crimp patterns disappear, which leads to a linear region with a higher stiffness. This combination of a toe region and a linear region ensures that the tissue can maximize efficiency in daily activities (low elongations) and resist excessive stretching during strenuous activities (high elongations). From this curve, structural properties, namely stiffness, ultimate load, ultimate elongation, and energy absorbed, are obtained.

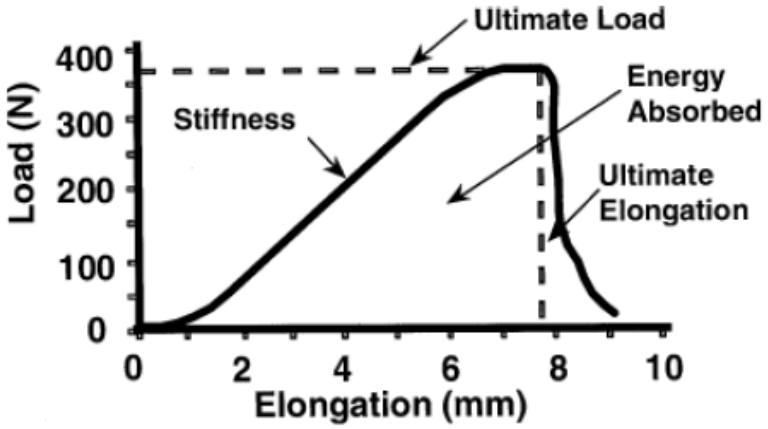

Figure A.1. A typical load-elongation curve from tensile testing of a ligament or a tendon.

Structural properties of a bone-ligament or bone-tendon complex is sensitive to the testing conditions. Specimen orientation during tensile testing, for example, has been shown to significantly affect the structural properties. When human femur-ACL-tibia complexes (FATC) were tested in an anatomical orientation where the angles of insertion at the femur and tibia are preserved, stiffness and ultimate load of FATCs were significantly higher compared those when tested in a non-anatomical orientation where it was aligned along the tibial axis (Woo et al., 1991). Using animal models, including the dog (Figgie et al., 1986), pig (Lyon et al., 1989), and rabbit (Woo et al., 1987b), specimen storage method (Woo et al., 1986) and testing temperature (Woo et al., 1987c), as well as donor age (Woo et al., 1991) and activity level (Larsen et al., 1987; Woo et al., 1982) were also found to be significant factors affecting structural properties.

2.1.2.2 Mechanical Properties of Ligament or Tendon Substance

Mechanical properties represent the intrinsic tissue quality irrespective to the dimensions of the tissue. As such, to obtain mechanical properties, normalization by the specimen dimensions is

needed. Load is normalized by the cross-sectional area of the specimen, resulting in stress. Elongation is normalized by the initial length of the specimen, leaving strain. By normalizing with the dimensions of the specimen, the values become independent of the specimen dimensions. From the stress-strain curve (see **Figure A.2**), tangent modulus, tensile strength, ultimate strain, and energy density can be obtained.

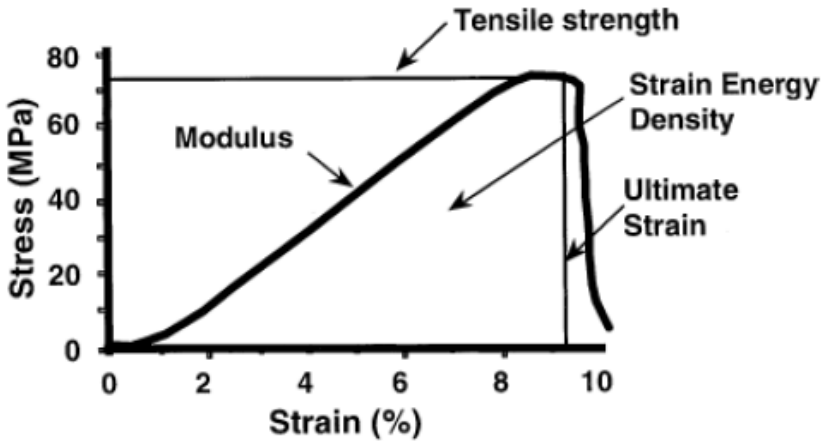

Figure A.2. A typical stress-strain curve from tensile testing of a ligament or a tendon.

To obtain mechanical properties, it becomes essential to obtain an accurate measurement of cross-sectional area of the ligament. Measuring cross-sectional area of a ligament or tendon is not a trivial matter as their shape is complex and physical contact (e.g. using a mechanical caliper) can distort its contour. It is thus important to utilize a non-contact method, such as an optical method, e.g. a laser micrometer (Woo et al., 1990).

2.1.3 Role of Ligaments and Tendons in Joint Function

It is also important to understand the function of ligaments and tendons in the context of the whole joint in addition to their behavior under uniaxial tension in isolation. In the past, linkage systems were used to study the contribution of ligaments and tendons on knee joint junction. However, these systems could not accurately record and replay kinematics in 6 degrees of freedom (Hollis et al., 1991). The robotic/UFS testing system was an improvement over the linkage systems as it can operate in full 6 degrees of freedom and has high precision in both kinematics and forces. This allowed direct comparison between multiple states (e.g. intact, ACL-deficient, and ACL-reconstructed) in a single joint, yielding high statistical power. With this system, functions of many ligaments and tendons have been studied, including ACL (Gabriel et al., 2004; Livesay et al., 1995) and PCL (Fox et al., 1998).

Using the robotic/UFS testing system, data on kinematics and forces in diarthrodial joints can be accurately measured in 6 degrees of freedom, i.e. forces and moments along three Cartesian axes as well as translations and rotations, in response to an externally applied load. The recorded kinematics data can then be accurately replayed to the same joint in different states. For example, the knee joint with an intact ACL can be subjected to an anterior tibial load, and the resulting kinematics and forces are recorded. The ACL is then resected, and the recorded kinematics is replayed. The difference in forces between the intact state and the ACL-deficient state is the force carried by the ACL or the in situ force. Then, an anterior tibial force can be applied again to the ACL-deficient joint to obtain the kinematics of an ACL-deficient joint. After ACL reconstruction, the same load is applied to obtain the kinematics of the ACL-reconstructed joint. The in situ forces in the ACL graft can be obtained in a similar manner as done for the

intact ACL. All procedures can be performed on a single joint, allowing direct comparison between different states.

2.2 LIGAMENT AND TENDON INJURIES AND CLINICAL MANAGEMENT

Ligament and tendon injuries are common with the estimated 800,000 surgeries performed each year (AAOS, 2008). Among these injuries, rotator cuff tears are the most significant problem in the upper extremity (Breazeale and Craig, 1997; Cotton and Rideout, 1964; Fukuda, 2000; Fukuda et al., 1994). Estimated 300,000 surgeries were performed to repair rotator cuff tears (Colvin et al., 2012). In the lower extremity, the ACL is one of the most frequently injured ligament with more than 100,000 cases per year. Two thirds of these cases would eventually require ACL reconstruction.

2.2.1 Anterior Cruciate Ligament

2.2.1.1 Anatomy and Function of Anterior Cruciate Ligament

The anterior cruciate ligament is an important knee stabilizer that provides restraint against anterior translation of the tibia respect to the femur and resistance against excessive internal-external rotation (Rudy et al., 1996; Woo et al., 1999b). The femoral insertion of the ACL is located at posterior side of the medial surface of the lateral condyle inside the intercondylar notch. The femoral insertion is observed as an oblong shape with the major axis aligned in the superoinferior axis. The ligament crosses (hence the name "cruciate") the midline of the femur and inserts to the tibia on anterior portion of the tibial plateau. The tibial insertion is longer in the anteroposterior direction than the mediolateral direction.

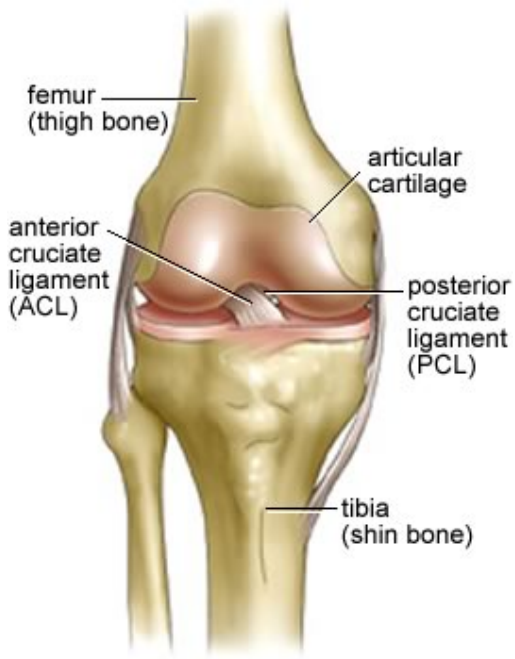

Figure A.3. Anatomy of the knee joint (shown as the right knee): Anterior cruciate ligament is showing in the middle as a white fibrous tissue between the femur and tibia.

(http://www.femaleathletesfirst.com)

The main role of the ACL in providing stability to the knee joint is to resist against anterior translation (Fujie et al., 1995) and valgus rotation (Inoue et al., 1987) of the tibia respect to the femur. It was found that with an increasing anterior drawer force (anterior force applied to the tibia), the load carried by the ACL increased (Fujie et al., 1995). This load is carried by two distinct bundles of the ACL, namely anteromedial (AM) and posterolateral (PL) bundles. In high extension (> 15°), the PL bundle takes up significantly larger loads than the AM bundle in response to an anterior tibial load (Sakane et al., 1997). With increasing flexion angle, contribution of the PL bundle significantly decreases while contribution of the AM bundle is relatively constant across all flexion angles, switching their roles in deep flexion. The two

bundles also differ in their role in resisting rotatory loads in near full extension. Under a combined rotatory load of valgus and internal torques, the AM bundle was loaded more than the PL bundle (Gabriel et al., 2004).

2.2.1.2 Epidemiology and Clinical Management of ACL Injury

Well over 100,000 cases of ACL injury occur each year in the US (Beaty, 1999; Miyasaka et al., 1991), making it the most injured knee ligament. It is estimated that $1 billion is spent each year to treat these injuries (Cole et al., 2005). ACL injuries are more prevalent in women. It has been shown that female athletes are three times more likely to injure their ACL during both contact and non-contact sports (Agel et al., 2007). This observation has been attributed to female athelete's tendency to stiff landing (Schmitz et al., 2007), but careful biomechanical analysis of in vivo drop landing using a biplane fluoroscope has not been able to substantiate this (Myers et al., 2011).

In the past, ACL injuries were managed with conservative treatment (Noyes et al., 1983; Walla et al., 1985). However, after a slew of follow-up studies showing unsatisfactory results (Kannus and Jarvinen, 1987; Pattee et al., 1989; Satku et al., 1986), failure has been attributed to the inability of a mid-substance tear of ACL to heal spontaneously (Hefti et al., 1991; Murray et al., 2000). Suture repair techniques have been attempted to help the healing by reapproximating the torn ends; however, no significant improvements were achieved over conservative treatments (Andersson et al., 1989; Kaplan et al., 1990). Finally, ACL reconstruction by replacing the torn ACL with a replacement autograft or allograft has become the treatment of choice to restore the knee stability.

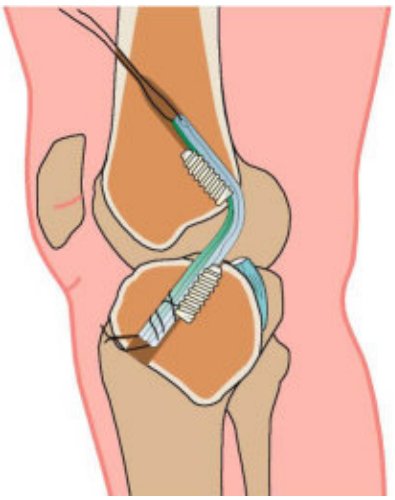

Figure A.4. ACL reconstruction using a hamstrings tendon. Polymer screws are used to fix the graft in both the femoral and tibial tunnels. (Source: http://www.londonkneeclinic.com)

The two most popular grafts to replace an injured ACL are the bone-patellar tendon-bone (BPTB) or hamstrings tendon (HT) grafts (Aglietti et al., 2004). Recently, there has also been renewed interest in the use of quadriceps tendon (QT) as an alternative graft choice besides the most popular two (Chen et al., 2006; DeAngelis and Fulkerson, 2007; Geib et al., 2009; Sasaki et al., 2014). The BPTB graft has been preferred by many because it has a high strength (Noyes et al., 1984). Also, it has bone blocks on both ends that could facilitate initial fixation in the bone tunnels and good osteointegration. Follow-up studies have shown good short- to mid-term outcomes after ACL reconstruction with a BPTB graft (Beynnon et al., 2002; Feller and Webster, 2003; Spindler et al., 2004). However, post-operative complications, such as patellar tendon ruptures, arthrofibrosis, loss of quadriceps function, anterior knee pain, and extension deficits, are still remaining problematic (Jarvela et al., 2000; Kartus et al., 2001). Hamstrings tendon grafts have been used as an alternative as it can address some of the complications associated with the BPTB graft, such as anterior knee pain and donor site morbidity. Further the graft

harvest is easier and requires smaller incisions. However, ACL reconstruction with HT grafts have shortcomings, such as increased knee laxity (Barrett et al., 2002; Beynnon et al., 2002), weakened knee flexors (Beynnon et al., 2002; Nakamura et al., 2002), and poor osteointegration (Segawa et al., 2001). Regardless of which graft is used, the most significant issue is long-term prevalence of osteoarthritis (Daniel et al., 1994; Drogset et al., 2006; Jomha et al., 1999; Selmi et al., 2006).

Animal experiments in dogs, pigs, and goats lend some insight to the causes of the poor outcomes of ACL reconstruction in longer terms. In general, there was a significant increase in anterior laxity within only few weeks (healing phase) after ACL reconstruction (Abramowitch et al., 2003; Fleming et al., 2009; Ng et al., 1995; Papageorgiou et al., 2001; Tomita et al., 2001; Weiler et al., 2002; Yoshiya et al., 1987), although initial joint stability could be restored (Abramowitch et al., 2003). Also, by 6 weeks, the stiffness of the healing BPTB graft was only 13 ~ 30% of the normal ACL (Abramowitch et al., 2003). These results indicated that although initial fixation may be adequate, healing of the graft reduces its function significantly. Thus, improving the healing of the graft would yield better overall outcomes for current ACL reconstruction techniques.

Healing of the ACL replacement graft depends on many factors, including fixation of the graft, biocompatibility of the implant material, and so on. Much effort has been given to optimize techniques and devices to fix the graft. Among many fixation devices developed and used, interference screws have been the longest used (Kurosaka et al., 1987; Lambert, 1983) and the most effective, as it provides sufficient pull-out strength and allows for fixation close to the joint space, reducing graft motion in the tunnel compared to suspensory mechanisms (Hoher et al., 1999). In an effort to improve biocompatibility of fixation devices and enhance bone healing,

recently, polymer-based interference screws have been introduced as it can degrade and let the native tissue to take over the function. Unfortunately, polymer-based interference screws had many complications, including fracturing during implantation, unpredictable degradation rates, and poor osteointegration (Smith et al., 2003; Stahelin et al., 1997; Walton and Cotton, 2007).

2.2.2 Rotator Cuff

2.2.2.1 Anatomy and Function of Rotator Cuff

The rotator cuff is a group of tendons that surrounds the glenohumeral joint to keep the humeral head on the glenoid. The four tendons are those of supraspinatus, infraspinatus, teres minor, and subscapularis muscles (see **Figure A.5**). Supraspinatus tendon attaches to the superior medial facet of the greater tuberosity. Infraspinatus tendon attaches to the posterior surface of the greater tuberosity. Teres minor attaches to the inferior face of the greater tuberosity. Subscapularis attaches at the lesser tuberosity.

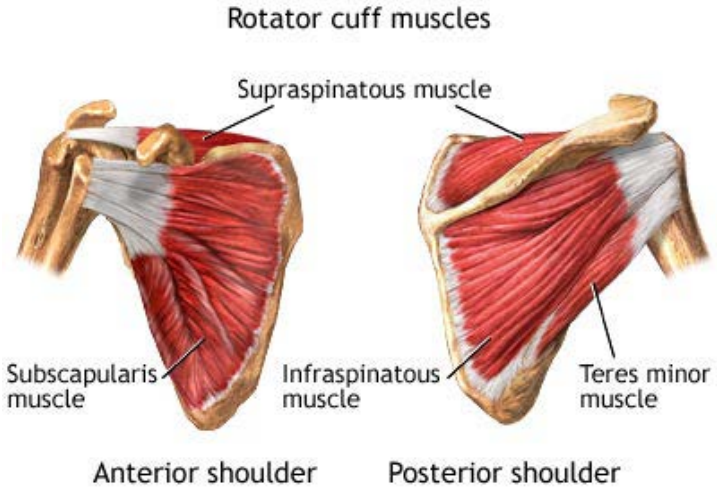

Figure A.5. Rotator cuff muscles. (Source: http:321gomd.com)

The rotator cuff provides stability to the glenohumeral joint mainly through active contraction of the muscles, thereby increasing the "concavity compression" on the glenoid (Lippitt et al., 1993). This compression provides resistance to excessive motion of the joint. It was also found that without active participation of the muscles, the passive properties of the rotator cuff also provide significant contribution to the joint stability. Using the robotic/UFS testing system, it was found that the contribution of the passive properties of the rotator cuff was more than the joint capsule (Debski et al., 1999) in the posterior direction. Overall, the contribution of the rotator cuff was greater in the posterior direction than in the anterior direction.

2.2.2.2 Epidemiology and Clinical Management of Rotator Cuff Tear

Rotator cuff tear is one of the most frequently damaged soft tissues in the musculoskeletal system with 8-26% of the population having a full-thickness tear (Cotton and Rideout, 1964) and 13-37% having a partial thickness tear (Breazeale and Craig, 1997; Fukuda, 2000; Fukuda et al., 1994). As many as 300,000 surgeries are performed in the US to repair rotator cuff tears, and this number is rapidly increasing with the growing population of the elderly (Colvin et al., 2012). Many factors have been identified as potential factors leading to rotator cuff tears, including acromial impingement (Longo et al., 2008), overuse (Soslowsky et al., 2002), smoking (Baumgarten et al., 2010), aging, and so on.

Although conservative treatment may be appropriate for the patients with well preserved motion and function (Tanaka et al., 2010), surgical repair is required to reduce pain and regain shoulder function, especially for full-thickness tears (Neri et al., 2009). With the advent of arthroscopic rotator cuff repair in the 90s, suture anchors have become indispensible for fixation of the torn tendon on the humeral head (Gleyze et al., 2000; Snyder, 1997). A single row technique utilizes a single row of usually 2 suture anchors to attach the very end of the torn

tendon on the humerus. This technique was thought to fail to cover the anatomic footprint of the tendon attachment, potentially leading to poor healing (Apreleva et al., 2002; Meier and Meier, 2006b). This led to popularization of double row techniques where two rows of 2 suture anchors per row are used (Meier and Meier, 2006a). Some positive results were found in laboratory studies in terms of initial fixation strength with double row techniques (Ma et al., 2006; Meier and Meier, 2006a).

Despite technical improvements made with arthroscopy and double-row techniques, management of rotator cuff tears have proven difficult. Although partial tears could be repaired with good outcomes, re-tear rates after repair of massive rotator cuff tears have been significant (Bishop et al., 2006; Boileau et al., 2005). Double-row techniques, despite their advantages in initial fixation, have been shown to make minimal improvements in patient outcomes (Franceschi et al., 2007).

In the recent years, augmentation using overlaying patches has been tried to reduce re-tear. Xenogeneic extracellular matrix scaffolds have been the popular material for this application (Badylak et al., 2009). These scaffolds could be derived from various types of animal tissues, e.g. small intestine submucosa, urinary baldder, and so on (Badylak et al., 2009). Although some success has been achieved, their use as a mechanical augmentation has led to complications due to acute inflammatory responses (Malcarney et al., 2005; Zheng et al., 2005). In laboratory studies, potential causes have been identified as incomplete decellularization (Zheng et al., 2005) and cross-linking of the collagen matrix (Badylak et al., 2008). Recent efforts have focused on development of improved decellularization methods (Keane et al., 2012) as well as using these scaffolds as a biological augmentation rather than a mechanical augmentation (Badylak et al., 2008).

Recently, other means of biological augmentation have been utilized to improve the healing of a torn rotator cuff, including stem cells (Chen et al., 2011; Gulotta et al., 2009), platelet-rich plasma (Castricini et al., 2011), and growth factors (Chen et al., 2011). Chen et al. (Chen et al., 2011) combined periosteum progenitor cells with an injectable hydrogel laden with BMP-2. The hydrogel was then injected at the tendon-bone interface after rotator cuff repair in rabbits. They observed increased fibrocartilage and bone formation by 4 weeks and 8 weeks. Biomechanically, the hydrogel also improved the ultimate load of the tendon-bone interface compared to control. On the other hand, the use of platelet-rich plasma has been found to be ineffective in improving the surgical outcome of rotator cuff repair in humans (Castricini et al., 2011).

3.0 RATIONALE

Soft tissue fixation in orthopaedic surgery as in the cases of graft fixation in ACL reconstruction and repair of a torn rotator cuff is done using screw-like fixation devices, such as an interference screw or a suture anchor. These devices are currently made of either a non-degradable metal or a bioresorable polymer. These materials have some unique strengths: excellent mechanical properties and acceptable biocompatibility for metals; biodegradability and suitability with MRI for polymers. However, many complications have been reported in the literature with the current fixation devices made of these materials. Hence, an alternative to overcome these issues would be highly desirable.

3.1 COMPLICATIONS ASSOCIATED WITH CURRENT FIXATION DEVICES

3.1.1 Metallic Devices

A major advantage of metallic materials is their high mechanical properties (Gay et al., 2009; Li et al., 2010; Li et al., 2003), with the elastic moduli in the order of 100 GPa (Ho et al., 2010; Li et al., 2010), to provide good initial fixation strength. They have also been shown to have acceptable biocompatibility for osteointegration (Beevers, 2003; Brand et al., 2000; Suchenski et al., 2010a). Nevertheless, there are several issues associated with metallic materials. Because of their ferromagnetic nature, they can distort post-operative MRI images (Bowers et al., 2008;

Shellock et al., 1992) (see **Figure B.1**). Clinical studies have shown that the presence of these metallic interference screws can interfere and confound the interpretation of surgical results (Bowers et al., 2008; Venter et al., 2001). Also, due to their permanency, if subsequent surgeries are needed, e.g. revision ACL reconstruction surgery, these devices need to be removed, further complicating these already difficult operations (Brand et al., 2005; Shen et al., 2010; Weiler et al., 1999; Zantop et al., 2006). In pediatric patients, the extensive implantation of non-degradable metal devices is problematic, potentially causing growth restriction and skeletal morphological alteration (Yaremchuk and Posnick, 1995).

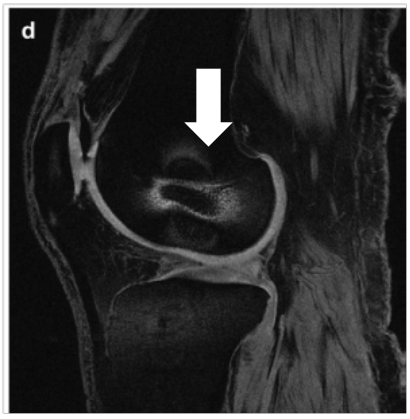

Figure B.1. MRI interference cause by a titanium interference screw used for ACL reconstruction. (Source: Bowers et al., 2008)

3.1.2 Polymer-Based Bioresorbable Devices

The disadvantages of non-degradable metallic devices have led to the development and increased use of bioresorbable polymer-based devices. They are advantageous since they would not distort MRI images. Further, since they are biodegradable, their removal is not required for a secondary surgery (Safran and Harner, 1996). In laboratory studies, polymer-based interference screws

have been shown to provide comparable initial fixation as titanium-based interference screws (Beevers, 2003). However, the rate of their degradation has been highly variable, ranging from almost complete resorption within one year to a significant presence at 4 years post-operatively (Ahmad et al., 1998; Bostman et al., 1992; Stahelin et al., 1997; Tay et al., 1999; Walton and Cotton, 2007). For these screws to degrade more quickly (<1 year), their initial mechanical properties have to be lower as a trade-off in material design. Their elastic moduli are generally 10 times lower than those for titanium alloys (Gay et al., 2009; Ho et al., 2010; Li et al., 2010) and leads to complications, like screw breakage during implantation (Barber et al., 1995; Lembeck and Wulker, 2005; Smith et al., 2003).

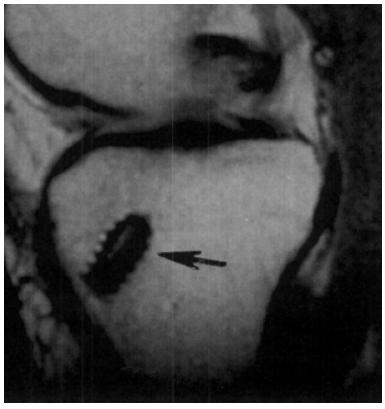

Figure B.2. Polymer interference screw is intact after 24 months as shown in MRI (arrow).

(Source: Barber et al., 1995)

Many have reported other complications, including migration of these bioresorbable screws into the intra-articular space following post-implantation breakage (Baums et al., 2006; Bottoni et al., 2000; Macdonald and Arneja, 2003; Shafer and Simonian, 2002) as well as inflammation (Boffa et al., 2009; Bostman et al., 1990; Kwak et al., 2008) that could contribute to poor osteointegration. Even with successful short-term results, bone tunnel widening and

incomplete filling of the tunnel could still occur in a significant portion of patients (Barber and Boothby, 2007; Fink et al., 2000; Laxdal et al., 2006; Moisala et al., 2008; Weiler et al., 2002). One study done at 10 year follow-up found that all patients had an osseous cyst in place of the degraded polymer screws (Ahmad et al., 1998).

Recently, biocomposite materials that are composed of polyester combined with ceramic particles (e.g., hydroxyapatite (HA) or β-tricalcium phosphate (β-TCP)), have been introduced to address the poor osteointegration of the bioresorbable polymeric screws (Garbern et al., 2011; Hunt and Callaghan, 2008; LeGeros, 2002; Lu et al., 2009; Macarini et al., 2008; Tecklenburg et al., 2006). However, their effectiveness has not yet been well demonstrated (Ahmad et al., 1998; Barber and Dockery, 2008). In a study using β-TCP-PLLA screws, only 10% of patients had complete filling of the bone tunnel following degradation of the screw (Myer et al., 2011). Furthermore, like polymeric materials, ceramics are extremely brittle, and thus, breakage during implantation remains a significant problem (Cojocaru et al., 2003).

3.2 A NEW CLASS OF MATERIALS − THE USE OF MAGNESIUM-BASED MATERIALS FOR ORTHOPAEDIC IMPLANTABLE DEVICES

3.2.1 History of Magnesium-Based Materials

The use of Mg-based materials for orthopaedic applications started in the early 20th century (Witte, 2010). The first successful application was for fixation of a humeral fracture using Mg nails. It was shown that although gas cavities formed around the implant, the fractured bone could heal. After this initial success, other applications followed, including pins for fracture fixation and pegs as intramedullary (Witte, 2010). In most cases, hydrogen evolution was significant but did cause inflammation or other adverse effects on the surrounding tissues. From

these initial studies, researchers learned that magnesium should not be used with other metals as they would lead to galvanic corrosion.

In the mid 20th century, larger scale clinical trials with Mg-based implants ensued, encouraged by the success in the earlier period. For example, Troitskii and Tsitrin successfully treated pseudarthrosis in 34 patients with screws and plates made of a Mg-Cd alloy (Witte, 2010). However, concerns of uncontrolled degradation and resulting gas cavities deterred most surgeons from adopting magnesium and its alloys for orthopaedic applications. Hence, more corrosion-resistant metals, such as stainless steel and titanium-based alloys have been introduced and dominated orthopaedics.

3.2.2 Advantages of Magnesium-Based Materials

3.2.2.1 Mechanical Properties

Mg alloys have appropriate mechanical properties over both polymeric materials and other non-degradable metallic materials, such as Ti-based alloys (Hort et al., 2010; Mantovani et al., 2003; Padua et al., 2009; Paramsothy et al., 2010; Staiger et al., 2006; Witte; Witte et al., 2005). Mg alloys have a modulus and tensile strength (41-45 GPa and 230-250 MPa, respectively) that is about 4-20 and 3-16 fold higher than PLLA polymers (2.2-9.5 GPa and 16-69 MPa, respectively). Plus, Mg alloys are much more ductile than polymeric materials, reducing the risk of brittle fracture. Thus, screws made from Mg alloys would yield better fixation strength and less risk of breakage during implantation. Meanwhile, the modulus and tensile strength of Mg alloys are 2-4 times lower than those of Ti alloys (110-117 GPA and 830-950 MPa, respectively) and more closely match those of cortical bone (3-20 GPa and 100-200 MPa, respectively). As such, this

novel material would reduce stress-shielding of the surrounding bone while still providing the needed fixation strength.

3.2.2.2 Controlled Degradation

Mg alloys can be designed to degrade at a desired rate (Mesfar and Shirazi-Adl, 2006; Padua et al., 2009). Animal studies reported that several Mg alloys implanted into the femur of guinea pigs have been degraded while a PLLA polymer showed very little degradation at 6 and 18 weeks post-surgery. On the other hand, the Mg alloy AZ31 had degraded about 30% and 70% at 6- and 18-weeks post-surgery, respectively. Recent work has also shown that the rate of degradation of Mg alloys can be controlled by including biocompatible alloying elements or through surface coating techniques (Liao et al., 2013) without compromising their initial mechanical properties.

3.2.2.3 Biocompatibility and Osteoinductivity

Mg alloys have been shown to be an biocompatible biomaterial (Padua et al., 2009; Waselau et al., 2007; Witte et al., 2006; Witte et al., 2005). When Mg alloy based substrates (AZ21) were placed within in-vitro culture conditions, they could support stromal cell adhesion and growth as well as differentiation toward an osteoblast-like phenotype. Further, Mg-based alloy shave been shown to be osteoinductive. When placed in-vivo in a rabbit model, Mg scaffolds (alloy AZ91D) was found to degrade together with enhanced formation of extracellular matrix and an increased rate of mineral apposition adjacent to it (Witte et al., 2007). In addition, an increased bone cell function that resulted in higher bone mass and a tendency to a more mature trabecular bone structure was found. When compared to a degradable polymer (SR-PLA96) in the femur of the guinea pig, Mg alloys (e.g. AZ31) showed higher mineralized bone formation at 6 and 18 weeks

post-operation (see **Figure B.3**) (Witte et al., 2005). In all cases, no adverse inflammatory response (e.g. fibrous tissue formation) has been observed.

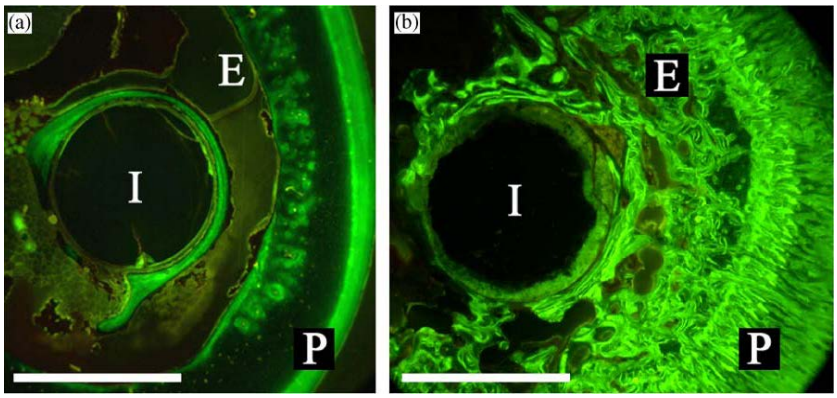

Figure B.3. In-vivo fluoroscopic staining of cross-sections of a degradable polymer (a) and a magnesium rod (b) in a guinea pig femur at 18 weeks. Bar=1.5mm; I=implant residual; P=periosteal bone formation; E=endosteal bone formation. (Source: Witte et al., 2005)

3.2.2.4 Suitability with Imaging Modalities

Mg-based alloys do not interfere with magnetic resonance imaging unlike other metallic materials, such as titanium or stainless steel alloys. Ernstberger et al. evaluated artefacts caused by Mg-based intervertebral discs and observed minimal interference by Mg-based discs (Ernstberger et al., 2010). In fact, the amount of artefact caused by Mg-based discs was comparable to that for polymer control. At the same time, Mg-based alloys can be imaged *in vivo* using computed tomography (Willbold et al., 2011) allowing accurate assessment of device degradation and bone formation.

3.2.1 Recent Developments in Magnesium-Based Materials

Recent developments in alloying, surface treatment/coating, and manufacturing have made it possible to modulate corrosion rates as well as mechanical and physical properties of Mg-based materials to tailor them for orthopaedic applications. Alloying elements for Mg-based materials can be those naturally occurring in the body, such as calcium (Ca), zinc (Zn), manganese (Mn), Fluorine (F), and so on. Zberg and co-workers demonstrated and the corrosion rate of magnesium can be modulated by changing contents of alloying components in a MgZnCa alloy without affecting its mechanical properties. This could make it possible to modulate the degradation rate of an implant to match the healing time of the injured tissue. Surface treatments can further fine-tune degradation of Mg-based materials. One of the most promising methods is calcium phosphate (Ca-P) coating (Ishizaki et al., 2009). With a simple immersion method, a Mg-based alloy AZ31 could be coated with Ca-P, and it could lower the degradation rate by 2 orders of magnitude.

Surface coatings not only improved degradation rates but also improved biocompatibility of Mg-based materials. Coating a MgMnZn alloy with Ca-P could significantly improve cell proliferation of mouse fibrosarcoma when used in vitro as a culture substrate (Xu et al., 2009). Functionalization of the surface of Mg-based materials has become also possible to improve biocompatibility. Kunjukunju et al. have demonstrated that a Mg-based alloy can be coated with PLLA-alginate (Kunjukunju et al., 2013). This surface could be conjugated chemically with fibronectic to vastly improve cell attachment.

To further enhance biocompatibility of Mg-based materials, methods have become available to modify their physical properties, such as porosity. For example, a porous Mg-CaP scaffold was created and implanted in femoral defects in rabbits (Wei et al., 2010). In 6 months,

the majority of the Mg-CaP scaffold had degraded and 81% of the defect was filled with re-grown bone, whereas with bone cement, only 47% of the defect was filled.

These improvements have clearly made Mg-based materials to have a greater potential to be used as a biodegradable material for orthopaedic applications. In fact, a human clinical trial is currently ongoing to test the use of a Mg-based screw for fixation of Hallux (Windhagen et al., 2013). It was demonstrated that Mg-based screws could achieve comparable fixation as a titanium control and achieve good bone healing. In the near future, more clinical applications of Mg-based materials are expected.

4.0 OBJECTIVES

4.1 BROAD GOALS

The overall objective of this dissertation is to develop screw-like devices made of a novel class of biodegradable metallic materials, namely using magnesium as an alternative because its desirable properties can effectively address shortfalls of the existing metallic and polymeric materials currently used to make these devices. First, since the Mg-based devices can be engineered to match their degradation profile to the healing process, the healing tissue can take over the function. Secondly, even though it is biodegradable, Mg-based devices would have good mechanical properties, reducing the risk of breakage. Lastly, the Mg-based devices will greatly enhance the treatment of pediatric orthopaedic population as it will not get in the way with the patient's growth. Mg-based interference screws for ACL reconstruction and Mg-based suture anchors for rotator cuff repair will be developed as examples. The development process and methods of evluation can then be used for other similar applications. Thus, at the completion of this dissertation, we hope to improve the clinical management of soft tissue injuries for both adult and pediatric patients significantly.

4.2 SPECIFIC AIMS AND HYPOTHESES

Specific Aim 1: Develop a Mg-based interference screw and test its feasibility for soft-tissue (bone-patellar tendon-bone graft) fixation in the bone tunnel for ACL reconstruction and evaluate its biomechanical function and biocompatibility at time zero and 12 weeks. Mg-based interference screws will be designed using finite element analysis (FEA) and preliminary in vitro testing. Mg-based interference screws will then be manufactured, and time-zero fixation of a bone-patellar tendon-bone graft for ACL reconstruction will be evaluated in goat stifle joints in terms of resistance to graft slippage upon cyclic loading and structural properties of the femur-graft-tibia complex. In vivo biomechanical performance for ACL reconstruction will be evaluated in a goat model at 12 weeks of healing period. The structural properties of the bone-graft-bone complex and restoration of joint function will be evaluated.

Hypothesis 1.1: A Mg-based interference screws of similar physical dimensions (diameter, length, and thread depth and pitch) as titanium screws would provide comparable initial fixation strength and stiffness as these dimensions have been shown to dictate fixation of a screw (Chapman et al., 1996).

Hypothesis 1.2: With good initial fixation of the graft confirmed in Hypothesis 1.1, the ACL reconstruction with a Mg-based interference screw will be able to restore joint stability as the in situ forces in the graft will be at the levels of the intact joint at time zero.

Hypothesis 1.3: After 12 weeks of healing, good biocompatibility is expected in terms of bone formation around the Mg-based interference screws. Osteogenic potential of the

Mg-based interference screws will accelerate osteointegration, leading to earlier and increased loading of the BPTB graft, thus helping with the graft incorporation that would ultimately lead to good graft function and joint stability.

Specific Aim 2: Design and manufacture a Mg-based biodegradable suture anchor for soft-tissue fixation, i.e. re-approximation of the torn rotator cuff on the humeral head in a rotator cuff surgery, and evaluate its biomechanical function at time zero. Using a similar design process as **Specific Aim 1**, Mg-based suture anchors will be designed and optimized using finite element analysis (FEA) and in vitro testing. Mg-based suture anchors will then be manufactured, and time-zero fixation will be evaluated in terms of pull-out strength and stiffness.

Hypothesis 2.1: By optimizing thread pitch and depth, the pull-out strength of Mg-based suture anchors can be improved as these parameters have been shown to dictate the pull-out strength of screw-like devices (Chapman et al., 1996).

Hypothesis 2.2: Mg-based suture anchors of similar physical design as polymer suture anchors would provide superior initial fixation strength compared to polymer-based suture anchors thanks to improved mechanical properties.

5.0 SPECIFIC AIM 1: MAGNESIUM-BASED INTERFERENCE SCREW

The goal of the Aim 1 is to demonstrate feasibility of Mg-based materials for soft-tissue-to-bone fixation in orthopaedic surgery by developing a Mg-based interference screw for ACL reconstruction and evaluating its biocompatiblity and biomechanical performance both *in vitro* and *in vivo*. The design of a Mg-based interference screw will be optimized by using finite element analysis to ensure secure fixation of the ACL replacement graft at time zero. Then, using the robotic/UFS testing system, joint stability and graft function after ACL reconstruction using Mg-based interference screws will be evaluated at time zero to test whether they can be restored close to the normal levels at time zero. Also, the femur-graft-tibia complex will be subjected to a uniaxial tensile test to ensure a Mg-based interference screw could provide good fixation of the replacement graft. At 12 weeks of healing, joint stability and graft function will be evaluated to test whether they are maintained compared to those at time zero. Uniaxial tensile testing will also be performed at 12 weeks to see if fixation is maintained and good graft integration has occurred.

5.1 GENERAL APPROACH

5.1.1 Design Optimization through Finite Element Analysis

Based on preliminary testing with prototypes based, issues with Mg-based interference screws were identified, namely screw stripping. A 3D model of Mg-based interference screw was built, and stress concentrations that led to those issues were identified in finite element analysis. To

alleviate this issue, drive depth and shape were varied in the finite element software and their effects on stress concentration in a Mg-base interference screw were investigated. Based on the findings of this analysis, optimal shape and depth for the screw drive were determined and Mg-based interference screws were manufactured.

5.1.2 In Vitro Evaluation of Mg-Based Interference Screw

In the second study, it was tested whether ACL reconstruction using Mg-based interference screws could restore joint stability and graft function at time zero. ACL reconstruction was performed on adult female Spanish goats in vitro using Mg-based interference screws to fix a bone-patellar tendon-bone autograft. (Abramowitch et al., 2003). Using the robotic/UFS testing system, anterior-posterior tibial translation (APTT) was measured in response to an anterior tibial load as a measure of joint stability. Also, in-situ force in the ACL and the replacement graft were obtained as a measure of graft function. To ensure that fixation of the replacement graft is secure, the femur-graft-tibia complex (FGTC) was subjected to a cyclic creep test to measure residual elongation and a load-to-failure test to obtain structural properties.

5.1.3 In Vivo Evaluation of Mg-Based Interference Screw

The third study was designed to test in vivo biocompatibility and biomechanical performance of Mg-based interference screws in a goat model. In vivo ACL reconstruction was performed on adult female Spanish goats with 12 weeks of healing period. 12 weeks was chosen as this is when the graft is going through remodeling and its mechanical properties are recovering from early inflammation and healing (Ng et al., 1995). Stifle joints were harvested and tested on the robotic/UFS testing system. The APTT (joint stability) and in situ forces in the graft (graft

function) at 12 weeks were obtained. The structural properties of the FGTCs were also obtained through uniaxial tensile testing.

5.2 METHODS

5.2.1 Initial Design of Mg-Based Interference Screw

The initial design of a Mg-based interference screw was based on the animal model used for *in vitro* and *in vivo* evaluation. The goat model was chosen based on its large joint size for ease of surgery and successful previous results with in vivo ACL reconstruction without complications (Abramowitch et al., 2003). Female Spanish breed goats between ages of 4 and 5 years were used because this strain of goats are less prone to disease and relatively easy to handle. Hindlimbs of goats of the same breed and age range were used for both time zero and in vivo evaluation. This allowed for comparison between time zero and later time points.

The optimal dimensions of a Mg-based interference screw for the goat model were determined as 5 mm by 15 mm (see **Figure C.1**). This size was optimal to match a 6 mm-wide bone-patellar tendon-bone (BPTB) graft, an optimal graft size to minimize the risk of patellar tendon failure and, at the same time, achieve good fixation. Previously, in vitro goat ACL reconstruction using a BPTB graft fixed with a titanium interference screw of the same dimensions achieved good fixation (Musahl et al., 2003). The screw drive was 3 mm deep and had a hexagonal shape.

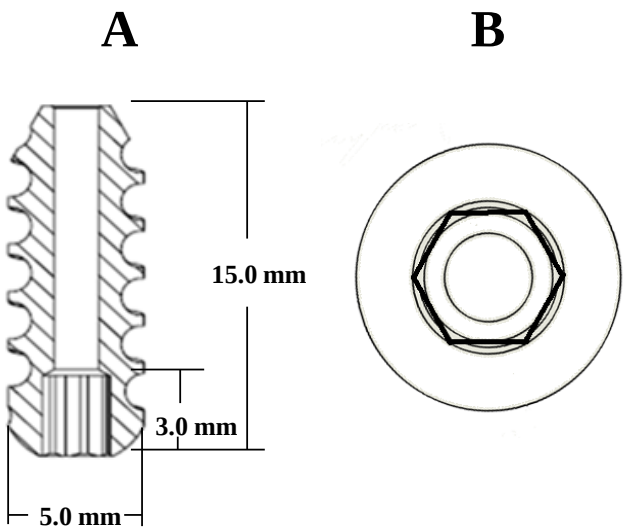

Figure C.1. Initial design of Mg-based interference screw. A: Dimensions (length, diameter, and drive depth). B: Hexagonal drive.

Prototype Mg-based interference screws were first made with pure magnesium, and preliminary testing was performed by fixing a bone-patellar tendon-bone graft in a femoral bone tunnel in 10 goat femora. From this, it was found that a Mg-based interference screw made of pure magnesium was not strong enough to withstand the torque required to insert the screw properly in the tunnel to provide good interference fit. The issue was attributed to the failure of screw drive leading to screw stripping (8 out of 10 trials). Thus, a switch to alloy AZ31 (aluminum 3 wt-% and zinc 1 wt-%) was made as it provided improved mechanical properties. AZ31 was also shown to be more corrosion resistant compared to pure Mg (Inoue et al., 2002). Mg-based interference screws manufactured with AZ31 alleviated the screw stripping problem.

5.2.2 Uniaxial Tensile Testing of Initial Mg-Based Interference Screw

Mg-based interference screws with the above dimensions were manufactured with AZ31. In order to ensure that they can be used for ACL reconstruction, preliminary in vitro testing was performed. Stifle joints of adult Spanish goats were obtained from an approved animal vendor. The specimens were stored in -20°C and thawed overnight before testing. All soft tissues on the tibial and femoral shafts were removed with only the soft tissue in and around the joint intact. The tibia and femur were then embedded in an epoxy material. A 5-mm wide bone-patellar tendon-bone graft was harvested. 6-mm wide bone tunnels were created on the femoral and tibial footprints of the ACL. The graft was placed in the tunnels and fixed with Mg-based interferences on both sides. All surrounding soft tissues were removed around the joint leaving just the femur-graft-tibia complex (FGTC). The FGTC was mounted on a materials testing machine and subjected to a uniaxial tensile testing as described in **section 5.3.2**.

5.2.3 Finite Element Analysis of Mg-Based Interference Screw

To address screw stripping of the Mg-based interference screw, finite element analysis was performed with the initial design of Mg-based interference screw using ANSYS 14.5 (ANSYS, Canonsburg, PA). First, 3D model of a Mg-based interference screw was constructed. The 3D model was embedded in a bone block (polyurethane foam, $E = 57.0$ MPa, $\upsilon = 0.240$) to simulate a tensile test in the finite element analysis software (see **Figure C.2**). The model including the Mg-based interference screw and the bone block was meshed with tetrahedral elements and convergence was confirmed through convergence tests.

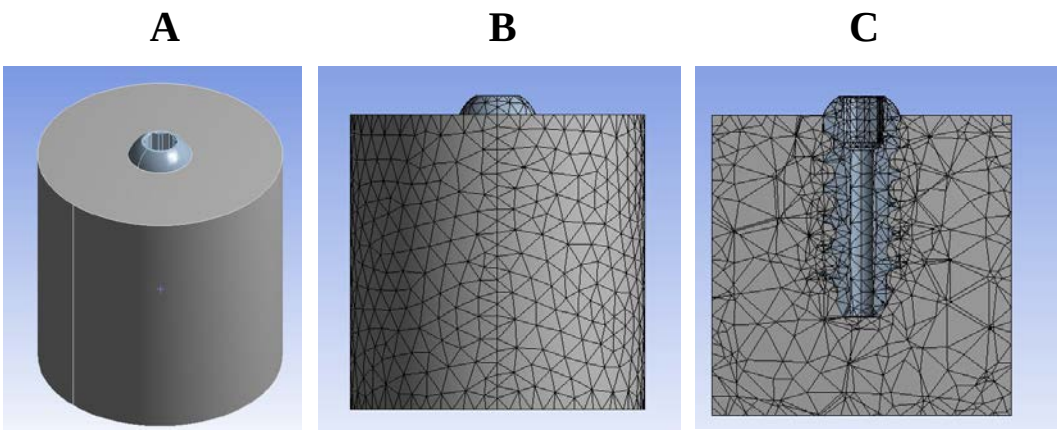

Figure C.2. 3D model of Mg-based interference screw embedded in a bone substitute material for finite element analysis. B: Outside view of meshed model. C: Cross-sectional view of meshed model. (Source: Flowers, 2013)

For model validation, the pull-out force of the Mg-based interference screw was determined with the following boundary and loading conditions. First, the bottom surface of the bone block was rigidly fixed. Displacements were applied to the top surface of the Mg-based interference screws embedded in the bone block as a loading condition to mimic a tensile test.

The maximum displacement was determined as a displacement value at which von Mises stress in either the mg-based interference screw or the bone block exceeds its shear strength. At the maximum displacement, pull-out strength of the Mg-based interference screw was calculated by summing reactions forces on the screw body. This value was compared to the value determined by a previously published equation that predicts the pull-out strength of a cancellous bone screw based on screw dimensions and thread design (Chapman, 1995) for validation.

Using the validated model, parametric optimization was performed. The purpose was to modify the screw drive design to reduce stress in the screw while a torque was applied to the drive for insertion. For this, shape and depth of the screw drive were varied parametrically to

determine the optimal values to minimize stress. The threads of the Mg-based interference screw were rigidly fixed to simulate friction with the surrounding bone during insertion. A 2 N-m torque was applied to the inner surface of the screw drive, and von Mises stress in the screw was determined. Optimal shape and depth of the drive that could reduce screw stripping were chosen for the finalized design to manufacture Mg-based interference screws.

5.2.4 In Vitro Evaluation of Improved Mg-Based Interference Screws

5.2.4.1 Surgical Procedure

ACL reconstruction using a bone-patellar tendon-bone autograft was performed through open surgery as described previously (Abramowitch et al., 2003). An anterior incision is made on the skin in the middle of the patella down to the tibial tuberosity. A 5-mm-wide BPTB graft was harvested with a 5 mm by 15 mm piece of bone taken from the patella and the tibia. The patellar end of the graft was armed with 2 Ethibond #2 sutures, and the tibial end was armed with a single Vicryl #2 suture. The ACL was completely resected, and a bone tunnel was drilled through its insertion site at the posterior portion of the femoral origin between 10 or 11 o'clock directions. On the tibial side, a bone tunnel was drilled at the anterior portion of the ACL footprint, with the opposite end exiting through the bony surface of the medial face of the tibia. The tibial end of the BPTB graft was pulled through the bone tunnels from the tibial opening. After placing the tibial end of the graft inside the femoral tunnel with the bone piece completely in the bone tunnel, a guide wire for screw placement was inserted next to the tibial bone piece of the graft. The graft was then fixed in the femoral tunnel by screwing in a Mg-based interference screw on top of its bony end, achieving interference fit. With 35 N tension on the graft, the joint was extended and flexed ten times. Fixation of the graft on the tibia was done with a double-

spiked plate and a staple with 35 N tension. Fixation of the graft was examined by performing a drawer test manually at various flexion angles. The patellar tendon was then sutured together to help healing, and the skin was sutured back together.

5.2.4.2 Methods of Evaluation

Robotic/UFS Testing System

The robotic/UFS testing system is an innovation developed and used in our research center for over two decades (Fox et al., 1998; Woo et al., 1999a). The robotic manipulator is capable of recording and reproducing the relative positions between the femur and tibia in the 3-dimensional space with an accuracy of less than 0.2 mm and 0.2º with full 6-DOF of motion. The UFS can measure three forces and three moments along and about a Cartesian coordinate system with an accuracy of less than 0.2 N and 0.2 N-m. In combination, the testing system can operate in force-control, position-control, and hybrid-control modes to gain information on joint kinematics as well as the forces carried by the ligaments.

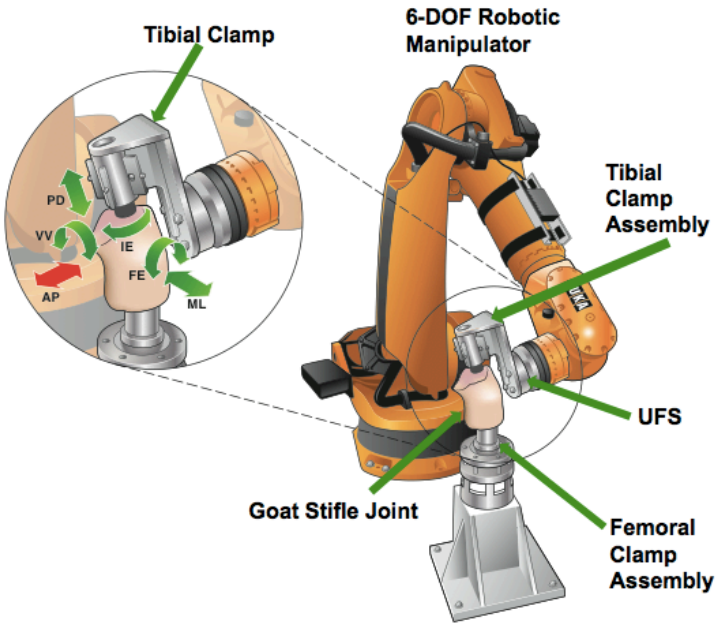

Figure C.3. 6 degree-of-freedom robotic/UFS testing system for joint kinematics and in situ force measurement. (Source: Farraro et al., 2014)

Goat stifle joint specimens were wrapped in saline soaked gauze and kept in - 20° C until the day prior to testing (Woo et al., 1986). After thawing at room temperature overnight, the tibial and femoral shafts were cleaned of any soft tissue with only the soft tissue in and around the joint intact and embedded in an epoxy material. The prepared specimen was then mounted on the robotic/UFS testing system.

The passive path was determined by flexing the joint at one degree interval from full extension to full flexion while minimizing forces and moments in the joint at each angle. This served as a reference position at each flexion angle. The intact joint was then subjected to a 67 N anterior-posterior (AP) tibial load. Resulting kinematics (K_I) and forces (F_I) were recorded at 30, 60, and 90 degrees of flexion. After dissecting the ACL (ACL-deficient state), the kinematics of the intact state (K_I) were replayed and the resulting forces (F_D) were recorded. In situ forces in

the intact ACL were obtained by subtracting F_D from F_I. In the ACL-deficient joint, a 67 N AP tibial load was applied, and the resulting kinematics (K_D) was also recorded.

ACL reconstruction was performed on the stifle joints as described in Section 5.2.2. The ACL-reconstructed joint (ACLR) was then subjected to a 67 N AP tibial load, and the resulting kinematics (K_R) and forces (F_R) were recorded. Afterwards, the replacement graft was removed, and K_R was replayed. The resulting force (F_{R-}) was subtracted from F_R to obtain in situ forces in the replacement graft. Anterior-posterior translations from K_I, K_D, and K_R were obtained as a measure of anterior-posterior stability of the joint.

Uniaxial Tensile Testing

With a femur-graft-tibia complex, uniaxial tensile testing was performed using a materials testing machine. After mounting the FGTC on a MTS, 3 N preload was applied; then, the specimen was preconditioned with 10 cycles between 0 and 1.5 mm of elongation at 50 mm/min. After an hour long recovery period, three cyclic loading tests were performed. In the first cyclic loading test, the femur-graft-tibia complex was loaded between 20 N and 70 N at 50 mm/min for 100 cycles. After another hour-long recovery period, the FGTC was loaded between 20 N and 105 N at the same extension rate with the same number of cycles. A higher load was chosen to simulate high intensity activities, such as running, as goats tend to be highly active even during the healing period. The third test was between 20 N and 70 N to see if the higher load in the second test had any lasting effect. At the end of the hour-long recovery period after each test, residual elongation, permanent non-recoverable elongation of the FGTC, was recorded.

After the cyclic loading tests, the FGTC was subjected to a load-to-failure test at 10 mm/min, and a load-elongation curve was recorded. From the load-elongation curves, stiffness

was calculated as the slope of the linear region of the curve and ultimate load and elongation were obtained.

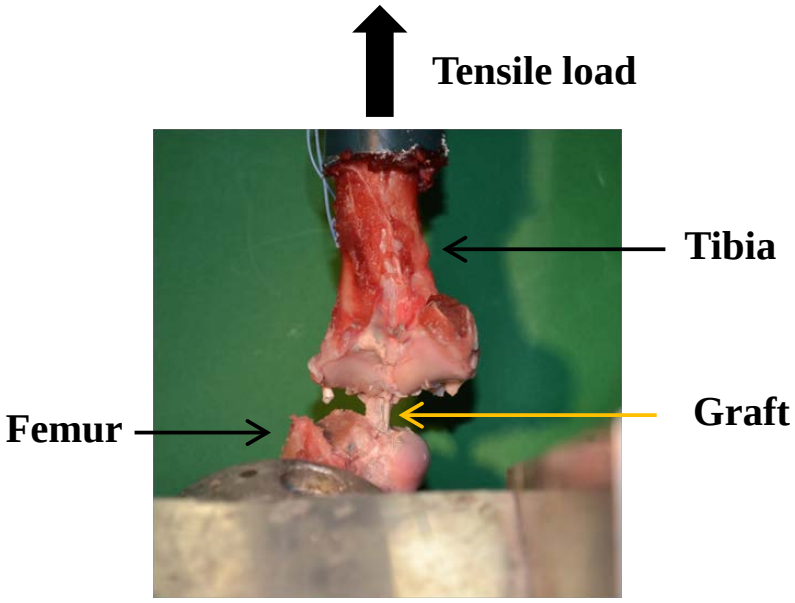

Figure C.4. Tensile testing of a femur-graft-tibia complex (FGTC). Femur is fixed in the bottom clamp, and the tibia is translated uniaxially to apply a tensile load to the FGTC.

5.2.5 In Vivo Evaluation of Improved Mg-Based Interference Screw

5.2.5.1 Surgical Procedure and Post-Operative Care

All surgeries were performed in compliance with the University of Pittsburgh IACUC policies using an approved protocol. All surgical procedures were performed using sterile techniques. The goats were pre-anesthetized with ketamine and intubated. Isoflurane gas anesthesia was used for the duration of the surgery. The right hindlimb served as the experimental group, while the left hindlimb served as a sham-operated control. On the left stifle joint, a medial incision was made to access the joint space and remove the fat pad. Then the incision was sutured close. This

was to isolate the experimental effects of the ACL reconstruction alone and reduce the potential effects of the surrounding tissues such as skin or fat pad. In the right hindlimb, an anterior midline skin incision was made to harvest a 6 mm wide central third patellar tendon graft complete with a small portion of the bone from the patella and tibia. Then the joint space was approached through medial incision.

The ACL was completely resected, and a 6-mm wide osseous tunnel was drilled through the posterior portion of the femoral insertion site of the ACL. The tibial tunnel was created on the tibial insertion of the ACL. The bone blocks of the bone-patellar tendon-bone (BPTB) graft to be passed through the femoral and tibial tunnels will be trimmed to snugly pass through a 6 mm sizer, respectively. The tibial bone block of the BPTB graft was placed in the femoral tunnel. A Mg-based interference screw was inserted in the bone tunnel next to the bone piece of the graft to provide a interference fit. Two size 2 sutures (Ethibond, Ethicon, Cincinnati, OH) were placed on the other end of the graft on the tendon substance. A double-spiked plate and screw (Smith and Nephews, Andover, MA) was attached to the graft using the sutures. With 35 N tension applied to the graft, the double-spiked plate and screw was fixed on the medial surface of the tibia. A bone staple was placed on the graft next to the spiked plate for additional fixation. The patellar tendon and skin were closed sequentially using resorbable sutures of size 2-0 (Vicryl 2-0, Ethicon, Cincinnati, OH).

Post-operatively, the goats were monitored daily for signs of pain and infection, as well as joint function (weight bearing and ambulation). X-rays were taken at 4 week intervals to ensure there is no serious complication, such as patellar tendon failure or bone fracture. At 12 weeks, they were euthanized humanely following an approved procedure, and the hindlimbs were harvested for testing.

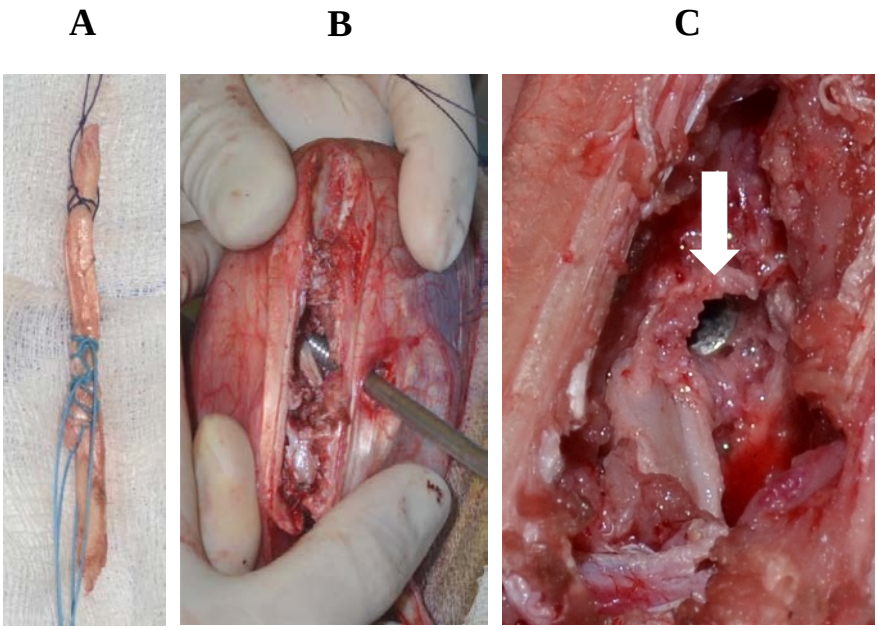

Figure C.5. Bone-patellar tendon-bone graft prepared with suture arms. B: A Mg-based interference screw is about to be placed in the femoral tunnel to fix the BPTB graft. C: A Mg-based interference screw (arrow) is driven all the way in the femoral tunnel. A white band of shiny tissue next to the Mg-based interference screw is the BPTB graft.

5.2.2 Methods of Evaluation

Robotic/UFS Testing System

The stifle joints harvested from the in vivo study animals were stored and prepared in a similar manner as the in vitro evaluation. The stifle joint was mounted on the robotic/UFS testing system and the passive path was determined. A 67 N AP tibial load was then applied to the joint, and the resulting kinematics (K_H) and forces (F_H) were recorded at 30, 60, and 90 degrees of flexion. Anterior-posterior translation from K_H was used as a measure of anterior-posterior stability of the joint. All soft tissues in and around the joint as well as bony contacts were removed, and K_H was

replayed. The resulting forces (F_G) were in situ forces in the replacement graft. The remaining femur-graft-tibia complex was subjected to uniaxial tensile testing immediately after.

Uniaxial Tensile Testing

With the femur-graft-tibia complex, uniaxial tensile testing was performed using a materials testing machine. A 3 N preload was first applied. The FGTC was then subjected to a load-to-failure test at 10 mm/min, and a load-elongation curve was recorded. From the load-elongation curves, stiffness was calculated as the slope of the linear region of the curve, and ultimate load and elongation were obtained.

5.3 RESULTS

In this section, results for Specific Aim 1 are presented. First, results from uniaxial tensile testing of the initial Mg-based interference screws will be discussed to show the need to improve the design. Then, results of the finite element analysis show how the issues with the initial design could be improved by modifying the drive design. The following *in vitro* evaluation of the improved Mg-based interference screw show whether they can be used for ACL reconstruction to restore initial joint stability and graft function. Also, results of tensile testing of the FGTC are presented to confirm good graft fixation. Finally, results of the *in vivo* evaluation at 12 weeks are presented and compared to those at time zero.

5.3.1 Uniaxial Tensile Testing of Initial Mg-based Interference Screw

2 out 4 Mg-based interference screws with the initial design made of AZ31 stripped during insertion to fix the graft. When stripped, the stripped screw was removed and another Mg-based interference screw was inserted as done during actual surgery. Total residual elongation of the Mg-based interference screws was significantly higher than that of a titanium interference screw after 3 cyclic tests (1.4 ± 0.4 mm vs. 4.0 ± 1.1 mm; $p < 0.05$; see **Table 1**). Interestingly, the stiffness was higher for Mg-based interference screws ($p < 0.05$), while the ultimate load was comparable. This indicated that the stripping problem with Mg-based interference screw may have prevented complete insertion in the tunnel. This presented a need to improve the screw design to eliminate screw stripping to ensure that the Mg-based interference screw could be fully inserted to provide good fixation.

Table 1. Residual elongation and structural properties of the FGTC with initial Mg-based interference screws and titanium screws.

	Mg-Based Screw (N = 4)	Ti Screw (N = 4)
Residual Elongation (mm)	4.0 ± 1.1*	1.4 ± 0.4
Stiffness (N/mm)	44.6 ± 7.3*	30.8 ± 11.3
Ultimate Load (N)	203 ± 18	211 ± 52

5.3.2 Finite Element Analysis of Mg-Based Interference Screw

With the model, convergence was achieved around 100,000 elements where the element size was 0.1 mm (see **Figure C.6**). With the initial design of Mg-based interference screw, upon applying

a 2 N-m torque to the hexagonal drive, it was found that stress concentrations arise at the six edges of the drive (see **Figure C.7**). Maximum von Mises stress was at these edges and it was 195 MPa. This was well above tensile strength of pure magnesium. Thus, this result corroborate the finding from preliminary testing that the initial Mg-based interference screws stripped during insertion. The change of material from pure magnesium to AZ31 alleviated this problem somewhat because tensile strength of AZ31 (250 MPa) was above the predicted maximum von Mises stress.

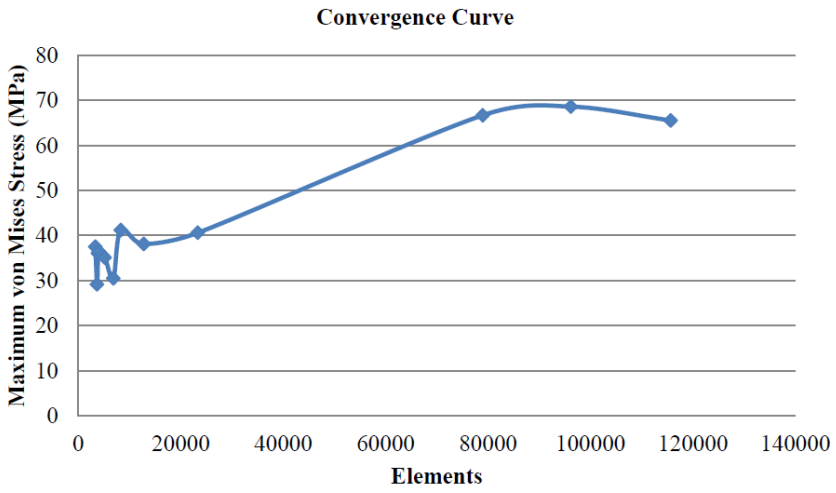

Figure C.6. Convergence curve of the finite element model based on maximum von Mises stress in the Mg-based interference screw. (Flowers, 2012)

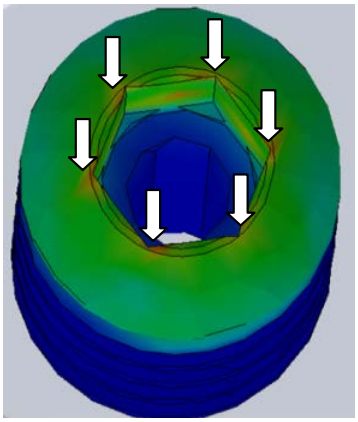

Figure C.7. Stress concentrations (at white arrows) at six edges of the hexagonal screw drive.

Comparison of various drive shapes revealed that a quadrangle (see **Figure C.8**) could make the edge of the drive substantially sharper without significantly increasing maximum von Mises stress compared to a hexagon (209 MPa vs. 195 MPa). This increased the amount of material that needed to be deformed before the drive would strip, i.e. to become circular. Other drive shapes, triangular, trilobe, torx, and turbine, could not be considered as with these shapes, it was difficult, if not impossible, to have a large enough cannulation in the driver to pass a guide wire through with the given dimensions of the Mg-based interference screw, which was an essential feature to perform ACL reconstruction.

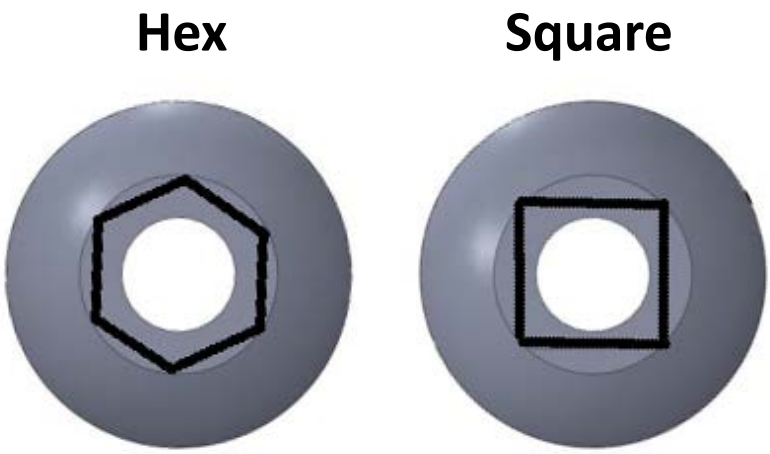

Figure C.8. Hex drive vs. square drive: With square drive, there is more material to resist stripping (i.e. drive becoming circular).

Increasing the depth of the screw drive had an inverse relationship with the maximum von Mises stress in the screw with a significant correlation ($R^2 = 0.90$). Up to 80% reduction in maximum von Mises stress was achieved by increasing the drive depth to 12.5 mm. Beyond this point, reduction was insignificant (< 5%). Based on these observations, the screw drive was made square and to span 12.5 mm of the entire length of 15 mm as this value was the maximum value where a significant benefit in reduced stress could be obtained. The final design is illustrated in **Figure C.9**.

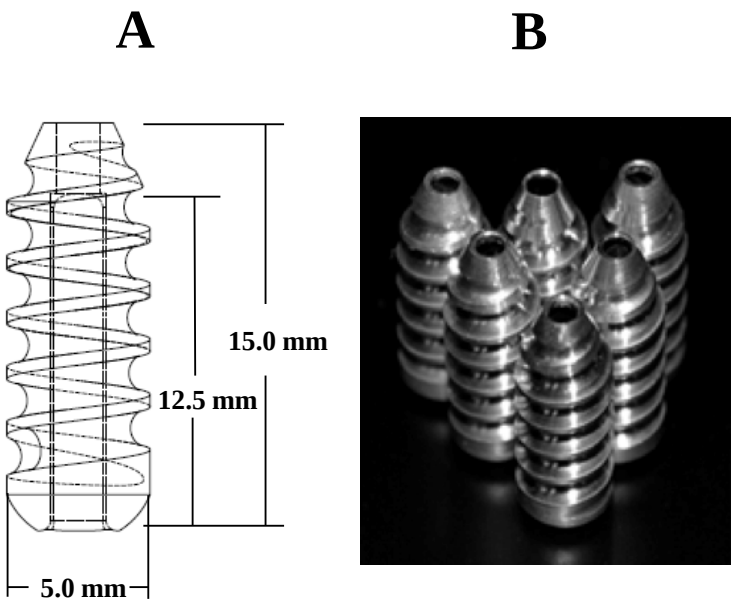

Figure C.9. A: Schematic of the improved design of Mg-based interference screw. 12.5 mm long drive (out of 15 mm total length) is indicated. B: Photograph of Mg-based interference screws manufactured with AZ31.

5.3.3 In Vitro Time Zero Biomechanical Evaluation

5.3.3.1 Joint Stability and Graft Function

The APTT in the intact joint was between 4.8 mm and 5.5 mm at 30, 60, and 90 degrees of flexion (see **Table 2**). This value increased by as much as 12 mm for the ACL-deficient joint, which was up to three times that for the intact joint (see **Figure C.10**). After reconstruction with a Mg-based interference screw, the APTT was reduced to within 1 mm of that of the intact joint, and these values were not significantly different (see **Table 2**; $p > 0.05$). The in-situ force in the replacement graft was between 51 N and 67 N (see **Table** 2). They were found to be within 5 N of that of the intact ACL at all tested angles (See **Table 2**), and they were not significantly different ($p > 0.05$; see Table 1).

Table 2. Anterior-posterior tibial translation (APTT) of intact, ACL-deficient, and reconstructed stifle joints and in situ forces in the ACL and replacement graft in response to a 67 N anterior-posterior tibial load at time zero.

Flexion angle (degree)	APTT (mm)			In-Situ Force (N)	
	Intact (N = 6)	ACL-deficient (N = 6)	Reconstructed (N = 6)	ACL (N = 6)	Graft (N = 6)
30	5.5 ± 0.9	17.9 ± 4.9*	6.1 ± 2.1	63 ± 13	67 ± 9
60	5.5 ± 0.9	17.5 ± 3.9*	6.2 ± 2.3	57 ± 6	60 ± 9
90	4.8 ± 0.8	15.6 ± 2.6*	5.5 ± 1.7	51 ± 6	51 ± 9

* Significantly different from all the other states at a given flexion angle ($p < 0.05$).

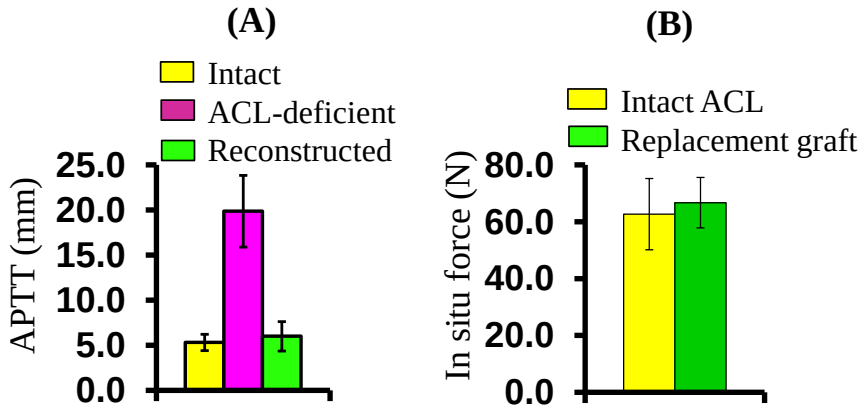

Figure C.10. (A) APTT and (B) in-situ force in response to a 67 N A-P tibial load at 30 degrees of flexion.

5.3.3.2 Uniaxial Tensile Testing of Femur-Graft-Tibia Complex

Residual elongation of the FGTC continued to increase up to 0.6 mm after two cyclic loading tests for the Mg-based screw group (see **Table 3**). For the titanium screw group, it increased to 0.8 mm after the first two cyclic tests. Between the second and third cyclic loading tests, residual elongation did not increase significantly for either group ($p > 0.05$), with the values at 7 mm and 8 mm, respectively. This indicated that residual elongation was converging to a stable value. When residual elongations of the two groups were compared, they were not significantly different after any of the three cyclic tests (see **Figure C.11**; $p > 0.05$).

The stiffness of the FGTC was 52 ± 6 N/mm for the Mg screw group and 50 ± 10 N/mm for the Ti screw group (See **Table 3**), and the difference was not statistically significant ($p > 0.05$). The ultimate load was 400 ± 135 N and 440 ± 109 N/mm, respectively, and they were not significantly different ($p > 0.05$). The ultimate elongation was 11.3 ± 2.6 mm and 13.1 ± 2.8 mm, respectively, and these values were not significantly different ($p > 0.05$).

Table 3. Residual elongation after the 1st, 2nd, and 3rd cyclic loading test and structural properties of the FGTCs from the load-to-failure test.

	Residual Elongation (mm)			Structural Properties		
	1st test	2nd test	3rd test	Stiffness (N/mm)	Ultimate Load (N)	Ultimate Elongation (mm)
Mg-Based Screw (N = 6)	0.3 ± 0.3	0.6 ± 0.6	0.7 ± 0.5	52 ± 6	400 ± 135	11.3 ± 2.6
Ti-Based Screw (N = 6)	0.3 ± 0.1	0.8 ± 0.3*	0.8 ± 0.3	50 ± 10	440 ± 109	13.1 ± 2.8

* Significant increase from the previous cyclic test

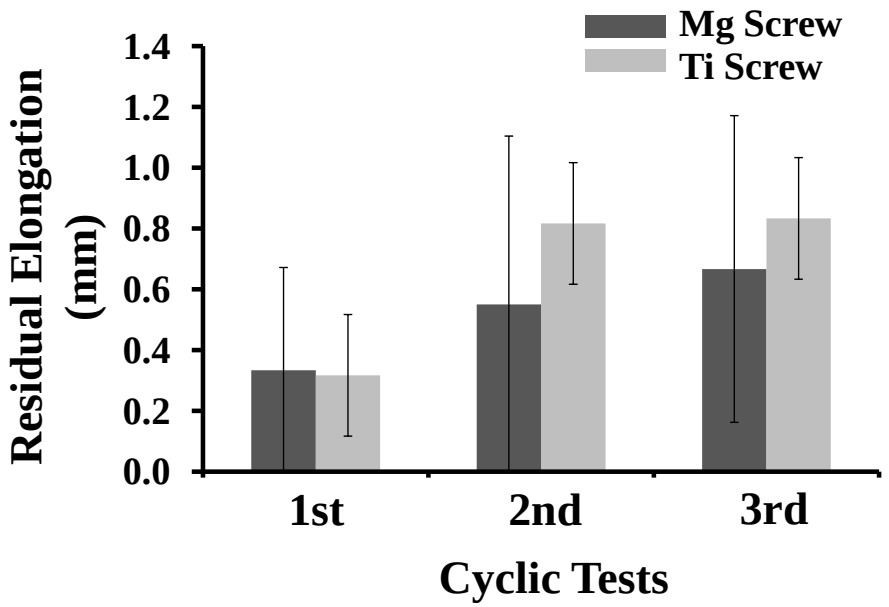

Figure C.11. Residual elongation after 1st, 2nd, and 3rd cyclic tests: Mg-based interference screw vs. titanium interference screws.

5.3.4 In Vivo Evaluation of Mg-based Interference Screws at 12 Weeks

5.3.4.1 Joint Stability and Graft Function

At 12 weeks, the goats could ambulate freely and run without any signs of limping, indicating that the joint function was recovered. Using the robotic/UFS testing system, the anterior-posterior tibial translations (APTT) in response to a 67 N APTL were found to be between 13.9 mm and 9.4 mm in the healing stifle joint (see **Table 4**). The APTT stayed constant between 30 and 60 degrees of flexion and decreased at 90 degrees of flexion. In situ forces in the healing graft were between 40 N and 20 N. It also stayed constant between 30 and 60 degrees of flexion and decreased at 90 degrees of flexion.

Table 4. Anterior-posterior tibial translation and in-situ force in the replacement graft immediately after ACL reconstruction (time zero) and after 12 weeks of healing.

	APTT (mm)		In-Situ Force (N)	
Flexion Angle (°)	Time Zero (N = 6)	12 Weeks (N = 6)	Time Zero (N = 6)	12 Weeks (N = 6)
30	6.1 ± 2.1	11.5 ± 3.1*	67 ± 9	38 ± 13*
60	6.2 ± 2.3	12.6 ± 2.2*	60 ± 9	35 ± 8*
90	5.5 ± 1.7	9.8 ± 2.9*	51 ± 9	22 ± 13*

*Significantly different from time zero ($p < 0.05$).

In comparison to the results at time zero, the APTTs at 12 weeks were significantly higher at all three angles ($p < 0.05$; see **Figure C.12**). The increased amounts were 5.4 mm, 6.4 mm, and 4.4 mm at 30, 60, and 90 degrees of flexion, respectively. The in-situ forces in the graft also decreased significantly at 12 weeks compared to those at time zero ($p < 0.05$; see **Figure C.13**). The decreased amounts were 29 N, 25 N, and 29 N at 30, 60, and 90 degrees of flexion, respectively.

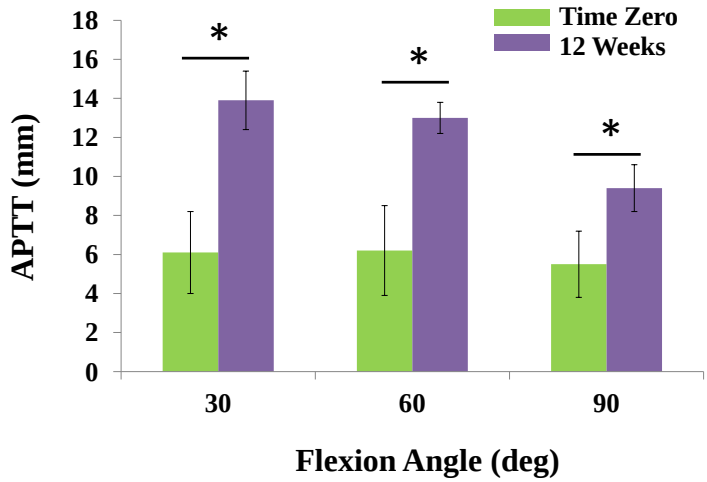

Figure C.12. Anterior posterior tibial translation (APTT) at 12 weeks (N = 6) vs. time zero (N = 6). *significant difference between the two time points ($p < 0.05$).

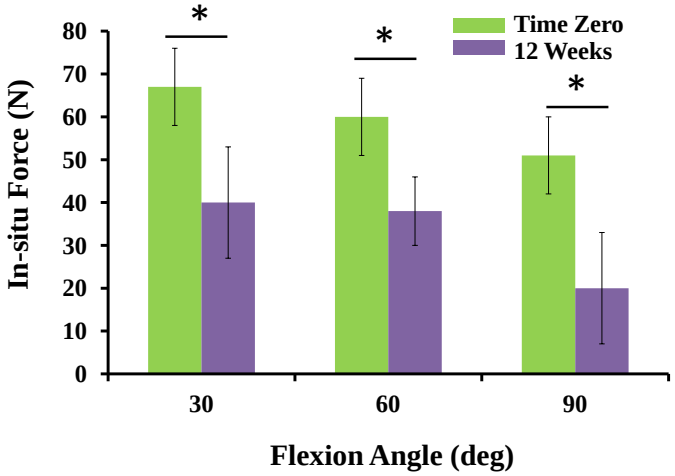

Figure C.13. In-situ forces in the ACL replacement at time zero (N = 6) vs. 12 weeks (N = 6). *significant difference between the two time points ($p < 0.05$).

5.3.4.2 Structural Properties of Femur-Graft-Tibia Complex

The load-elongation curve of the healing FGTC at 12 weeks was nonlinear similar to the shape of the load-elongation curve obtained with the normal ACL (see **Figure C.14**). The stiffness of the healing FGTC were 43 ± 11 N/mm, and this value was comparable to that at time zero ($p > 0.05$, see **Figure C.15**). The ultimate load was 261 ± 88 N, and there was no statistical difference from that at time zero ($p < 0.05$, see **Figure C.15**). The ultimate elongation was 7.0 ± 2.0 mm, and this was a 38 percent decrease from that at time zero (11.3 ± 2.6 mm) ($p < 0.05$).

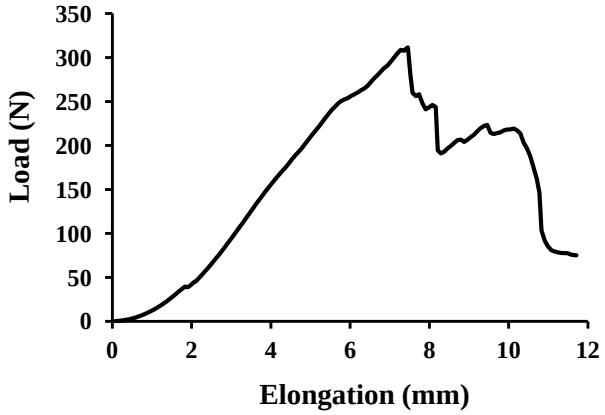

Figure C.14. Typical load-elongation curve of the femur-graft-tibia complex at 12 weeks.

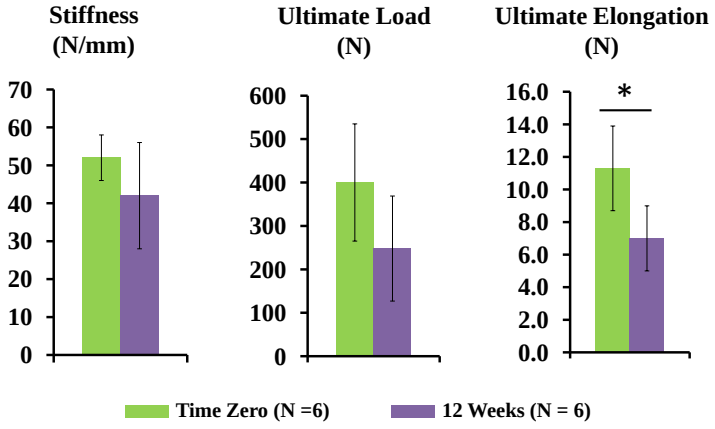

Figure C.15. Structural properties of the femur-graft-tibia complex at time zero (N = 6) vs. 12 weeks (N = 6). *significant difference between the two time points ($p < 0.05$).

6.0 SPECIFIC AIM 2: MAGNESIUM-BASED SUTURE ANCHOR

In Specific Aim1, *in vivo* biocompatibility and biomechanical performance of a Mg-based alloy for soft-tissue fixation was evaluated. Guided by the results of Specific Aim 1, Specific Aim 2 followed a similar process to design a Mg-based suture anchor for rotator cuff repair. First, using finite element analysis, the design of a Mg-based suture anchor will be optimized in a similar manner as done with the Mg-based interference screw. Mg-based suture anchors were then manufactured and in vitro biomechanical evaluation was performed at time zero through uniaxial tensile testing.

6.1 GENERAL APPROACH

6.1.1 Finite Element Analysis and Design Optimization

A Mg-based suture anchor was designed with dimensions determined from the literature for a surgical procedure of rotator cuff repair (Fealy et al., 2006). A preliminary tensile test was performed *in vitro*. With a 3D model of the Mg-based suture anchor, finite element analysis was performed to simulate the tensile test of the Mg-based suture anchor. The model was validated by matching the experimental data from the pull-out test. The validated model was then used to perform parametric optimization where the key factors that affect fixation, namely thread pitch and depth (Chapman et al., 1996), were varied, and their effect on von Mises stress in the screw

and the surrounding bone substitute material was investigated. Based on the results of the optimization, optimal values for the thread depth and pitch were chosen, and Mg-based suture anchors were manufactured accordingly.

6.1.2 In Vitro Evaluation of Mg-Based Suture Anchor

With the manufactured Mg-based suture anchors, a tensile test was performed to ensure that Mg-based suture anchors indeed achieve superior fixation strength compared to a polymer control. Mg-based suture anchors were inserted in a pre-drilled hole in a sheep humerus. A steel wire was placed as a replacement for a suture to ensure that there is no elongation other than displacement of the Mg-based suture anchor. This was also to eliminate suture failure as a failure mode, which could complicate comparison between different suture anchors. They were then subjected to a pull-out test in porcine femora to obtain pull-out force (ultimate load) and stiffness (Barber et al., 2008).

6.2 METHODS

6.2.1 Initial Design of Magnesium-Based Suture Anchor

The dimensions were based on the literature for the surgical model frequently used for rotator cuff repair so that the manufactured Mg-based suture anchors could be eventually used for in vivo studies (Fealy et al., 2006). The outer diameter and length were 6.5 mm and 16.5 mm, respectively (see **Figure D.1**). Thread pitch was chosen to be 3 mm to allow for quick insertion as with this will require only 5 turns. Thread depth was 1 mm. The suture eyelet was placed distally (toward the leading end) and the diameter was 1.5 mm to fit two size 2 sutures. The

suture tracks ran along the opposite sides with 0.8 mm depth and 1.5 mm width to fit two size 2 sutures (see **Figure D.1B**).

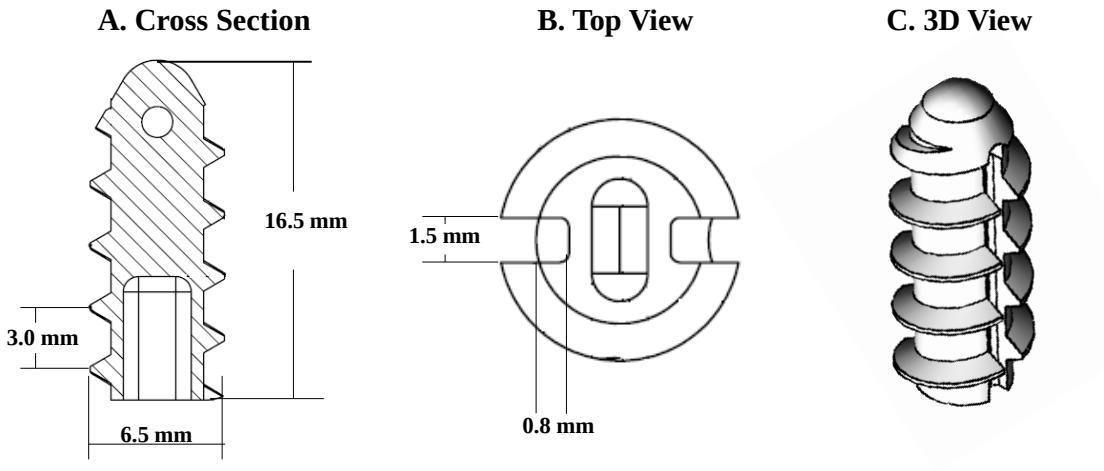

Figure D.1. Schematic of design of Mg-based suture anchor. A: Cross sectional view showing length and diameter, as well as thread pitch. B: Top view showing dimensions of the suture track. C: 3-dimensional view of suture anchor showing the thread and suture track.

6.2.2 Finite Element Analysis

3D model of a Mg-based suture anchor was built using SolidWorks (Dassault, Waltham, MA) (see **Figure D.2**) based on its dimensions described in Section 5.3.1.1. This 3D model was then embedded in a polyurethane foam to simulate the tensile test described in the previous section. This was done to validate the model by matching the experimental data from the pull-out test. The material properties for magnesium ($E = 9.60 \times 10^4$ MPa, $\upsilon = 0.360$) and polyurethane foam ($E = 57.0$ MPa, $\upsilon = 0.240$) were assigned respectively.

Finite element analysis was performed in ANSYS Workbench 14.5 (ANSYS, Canonsburg, PA). As a loading condition, displacements (0.05 mm, 0.1 mm, 0.2 mm, and 0.3 mm) below the failure point (determined from the pull-out test in section 5.3.1.3.) were applied

on the top surface of the suture eyelet to simulate the tensile testing conditions (i.e. a steel wire pulling on the suture anchor). For the boundary conditions, the bottom surface of the polyurethane foam block was rigidly fixed as in the tensile test. The contact surface between the Mg-based suture anchor and the polyurethane foam block was set to be a linearly frictional surface with a coefficient of friction of X.

For a convergence test, a displacement of 3 mm (ultimate elongation from the pull-out test in section 5.2.1.3.) was applied to the upper surface of the suture eyelet, and the reaction force was recorded with an increasing number of elements.

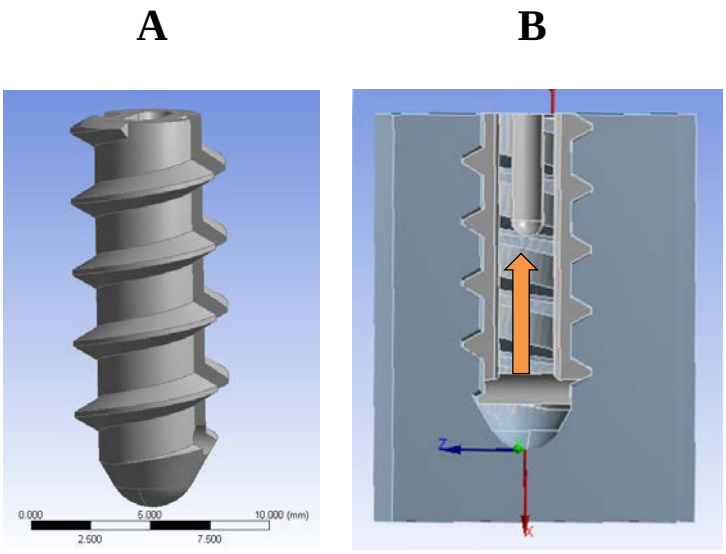

Figure D.2. 3D model of Mg-based suture anchor. B: Mg-based suture anchor embedded in polyurethane foam to simulate the pull-out test. Orange arrow shows tensile loading applied to the suture eyelet to simulate the loading condition.

Predicted von Mises stress in the model and the reaction force were recorded and compared to the experimental values obtained at these displacement values. By modifying the

parameters of contact between magnesium and polyurethane (as these were unknown), predicted values and experimental data were matched for validation.

6.2.3 Parametric Analysis of the Design of Mg-Based Suture Anchor

Using the validated model of Mg-based suture anchor, thread pitch and depth were varied parametrically to investigate their effects on maximum von Mises stress in the anchor or in the surrounding bone. Chosen values for thread pitch were 2, 2.5, and 3 mm, and the values for thread depth were 0.4, 0.7, and 1 mm. These values resulted in 9 different thread designs (see **Figure D.3**). The 9 modified models were analyzed using identical boundary and loading conditions as Section 5.3.1.3., and the resulting maximum von Mises stress was obtained at the prescribed displacement values.

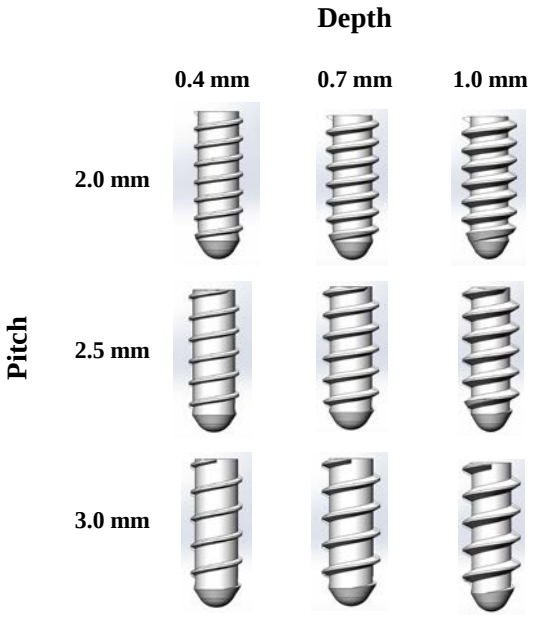

Figure D.3. 3D models of suture anchors of different dimensions used for parametric optimization.

6.2.4 Tensile Testing: Mg-Based Suture Anchor vs. Polymer Suture Anchors

A tensile test of prototype Mg-based suture anchors was performed to compare initial fixation of Mg-based suture anchors to that of commercially available polymer suture anchors. A hole with diameter 4.75 mm was pre-drilled on a precut block (13 cm x 4.5 cm x 4 cm) of a uniformly rigid polyurethane foam (15 pcf, SAWBONES, Vashon, WA). A polyurethane foam was used as this material is often used as a substitute for human bone in mechanical testing of orthopaedic implants . A braided steel wire, serving in place of a suture was passed through the distal eyelet of anchor to eliminate suture breakage as a possible failure mode, thus comparison can be made between different materials.

The anchor was inserted in the pre-drilled polyurethane foam. The two ends of steel wire were clamped to form a loop. The polyurethane foam with the Mg-based suture anchor was then mounted on a materials testing machine (Instron 5565, Instron, Norwood, MA), and the steel wire was clamped on the load cell. The Mg-based suture anchor was then pre-loaded to 50 N to straighten the steel wire. A load-to-failure was performed at an elongation rate of 50 mm/minute. A load-elongation curve was obtained. A total of 6 Mg-based suture anchors were tested. 6 polymer suture anchors of similar dimensions (Healio 6.5 mm, Depuy Mitek, Warsaw, IN) were used as a control.

6.3 RESULTS

In this section, results for Specific Aim 2 are presented. Based on the testing conditions of the tensile test, a finite element analysis was performed, and the computational data were matched to the experimental data for validation. Using the validated model, effects of the thread pitch and

depth on fixation of the Mg-based suture anchor were explored and the results are presented. Finally, *in vitro* biomechanical evaluation was performed at time zero by performing a tensile test in polyurethane bone block and compare the results to those of commercially available polymer suture anchors.

6.3.1 Finite Element Model of Mg-Based Suture Anchor and Validation

3D models were meshed using a quadratic tetrahedral element (see Figure X). With an increasing number of elements (i.e. decreasing element size), the predicted reaction force with 0.3 mm of displacement increased gradually (see **Table 5**). Convergence was achieved at 100,000 elements as variation was within 1% in three consecutive numbers of elements (see **Figure D.4**).

Table 5. Predicted reaction force (N) in response to 0.3 mm displacement applied to the Mg-based suture anchor with an increasing number of elements.

Number of Elements	Predicted Reaction Force (N)
19971	155.25
28725	151.82
38809	148.29
58592	143.01
98406	139.44
122528	137.02

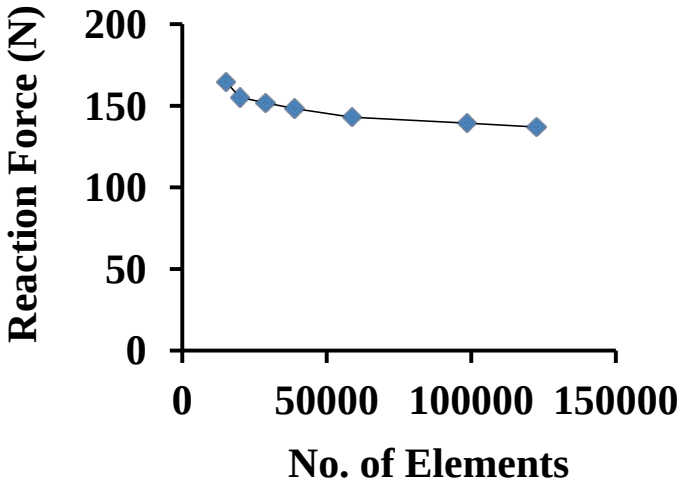

Figure D.4. Convergence curve of the Mg-based suture anchor model embedded in a polyurethane foam block with a displacement of 3 mm applied to the suture eyelet.

From the finite element analysis, the predicted reaction force from 22 N at 0.05 mm to 143 N at 0.3 mm (see **Table 6**), and it increased linearly with the displacement. Both the experimental load-elongation curve and the predicted load-elongation curve had a linear shape (see **Figure D.5**). The percentage difference between the predicted reaction force and the actual load was more than 200% (see **Table** 6).

Table 6. Predicted reaction force, average experimental data, and percentage difference at each displacement before subtracting the contribution of the steel wire.

Displacement (mm)	Predicted Reaction Force (N)	Average Experimental Data (N)	Percentage Difference (%)
0.05	22	7	214
0.1	46	14	229
0.2	95	32	197
0.3	143	53	170

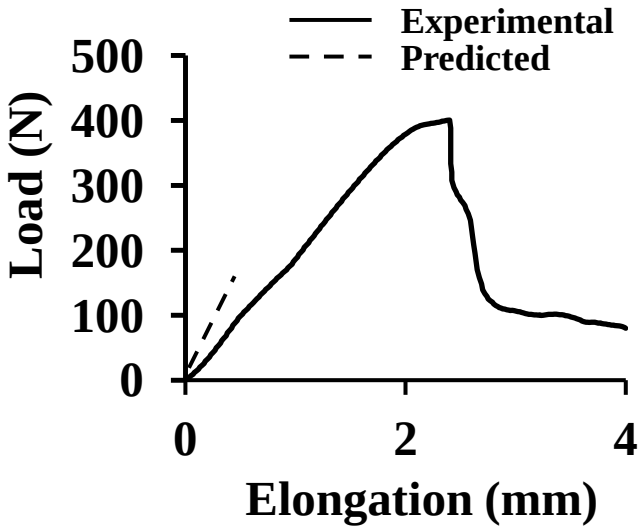

Figure D.5. A typical load-elongation curve of a Mg-based suture anchor from tensile test vs. the predicted load-elongation curve from the finite element model.

We then tested the steel wire itself as its presence lowers the stiffness of the entire construct of the wire and suture anchor. This was the case because the wire was in series with the suture anchor. The stiffness of the suture anchor itself embedded in the polyurethane foam block was then calculated using the following formula,

$$\frac{1}{K_{anchor}} + \frac{1}{K_{wire}} = \frac{1}{K_{combined}}$$

where K_{anchor} is the stiffness of the anchor alone, K_{wire} is the stiffness of the steel wire alone, and $K_{combined}$ is the stiffness measured in the experiment. K_{wire} was determined by performing a tensile test with only the steel wire. This value was 290 N/mm. From this, K_{anchor} was determined to be 510 N/mm. The predicted stiffness was 476 N/mm. The difference was less than 10%, validating the results of the finite element analysis.

6.3.2 Parametric Analysis of the Design of Mg-Based Suture Anchor

Upon applying the loading condition, Maximum von Mises stress in the suture anchor was located at the point where the first thread meets the suture eyelet (see **Figure D.6**). We then looked at von Mises stress in the polyurethane foam where its engaging the suture anchor as that was where failure occurred during tensile testing.

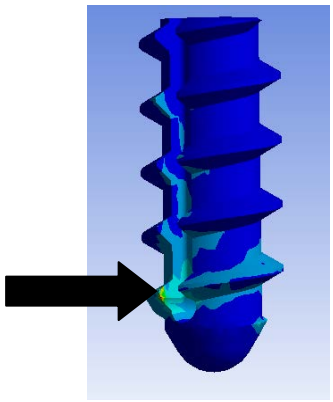

Figure D.6. Stress distribution in the PU foam in contact with the Mg-based suture anchor (3 mm pitch and 1 mm depth of thread) upon 0.3 mm displacement. Arrow points at the location of maximum von Mises stress.

Table 7. Maximum von Mises stress in the polyurethane block in contact with the Mg-based suture anchor with varying thread depth and pitch when 0.3 mm of displacement applied to the eyelet.

Thread Depth (mm)	Pitch = 2.0 mm (MPa)	Pitch = 2.5 mm (MPa)	Pitch = 3.0 mm (MPa)
0.4	14.1	15.8	14.1
0.7	10.8	12.9	12.8
1.0	10.5	12.6	16.6

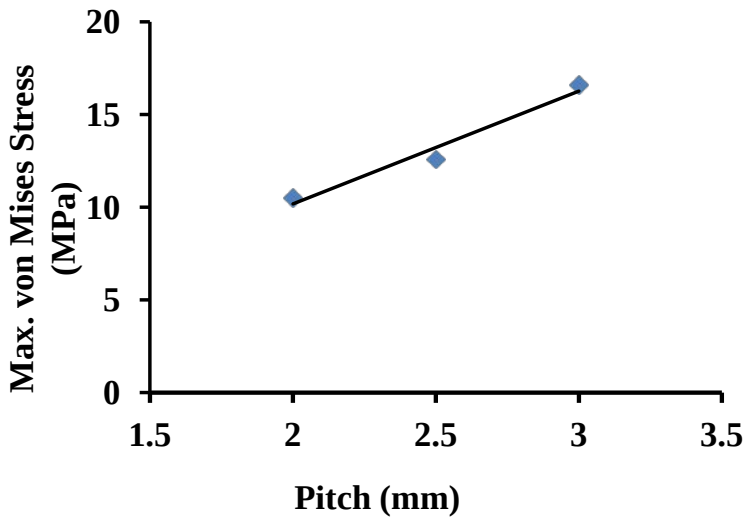

Figure D.7. Maximum von Mises stress in the finite element model vs. thread pitch with thread depth of 1.0 mm.

With increasing thread pitch, maximum von Mises stress in the polyurethane block increased by up to 50% (see **Figure D.7**), indicating a smaller thread pitch is better. Increasing the thread depth to 1 mm from 0.4 mm could reduce maximum von Mises stress by 30% (see **Figure D.8**). Although we found that these parameters could significantly affect the performance of the Mg-based suture anchor, our preliminary tensile test of the prototypes of Mg-based suture anchors indicated that its initial fixation was significantly better compared to that of polymer suture anchors. Thus, we continued with the initial design of the Mg-based suture anchors to perform further tensile testing to compare with polymer suture anchors.

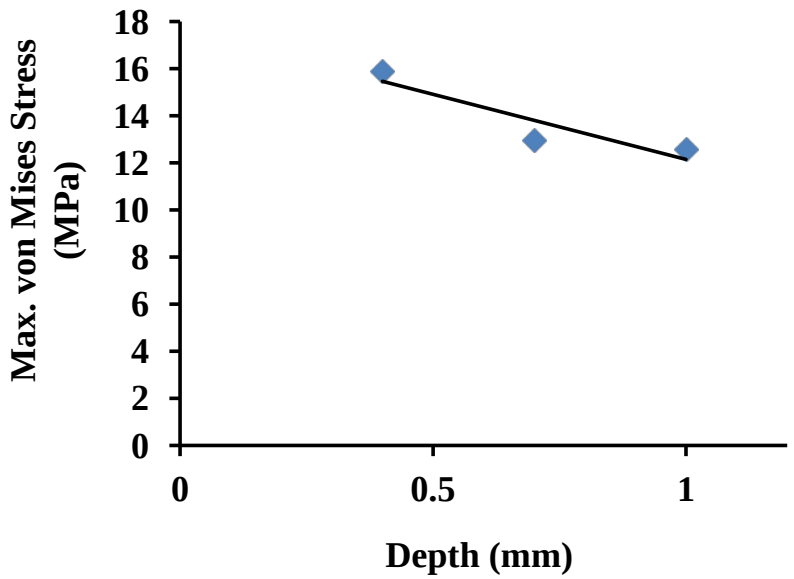

Figure D.8. Maximum von Mises stress in the finite element model vs. thread depth with thread pitch of 3.0 mm.

6.3.3 Tensile Testing of Mg-Based Suture Anchors

The load-elongation curves obtained with the Mg-based suture anchors were mostly linear up to the ultimate load (~ 400 N) (see **Figure D.9**). With the polymer suture anchors, the linear region was up to around 100 N, at which point yielding was observed. Stiffness was 185 ± 13 N/mm for Mg-based suture anchor group, and it was significantly higher compared to the polymer suture anchor group (107 ± 13 N/mm, $p > 0.05$). Ultimate load and elongation were also significantly different between the two groups ($p > 0.05$). For the Mg-based suture anchor group, failure occurred 100% through pull-out of the anchor from the foam block. For the polymer suture anchor group, failure only occurred through eyelet failure, i.e. the wire pulling out of the anchor.

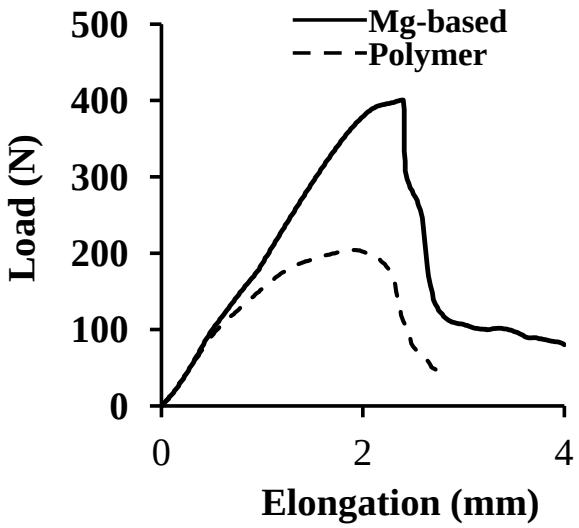

Figure D.9. Typical load-elongation curves from tensile testing of a Mg-based suture anchor and a polymer suture anchor.

Table 8. Structural properties of the suture-anchor-bone complex for Mg-based suture anchors and polymer suture anchors.

	Mg-Based Suture Anchor (N = 6)	Polymer Suture Anchor (N = 6)
Stiffness (N/mm)	185 ± 13*	107 ± 13*
Ultimate Load (N)	379 ± 34*	210 ± 13*
Ultimate Elongation (mm)	2.4 ± 0.2*	1.9 ± 0.2*
Failure Mode	100% pull-out	100% eyelet failure

*Significant difference between the two groups

7.0 DISCUSSION

In this dissertation, we have demonstrated that Mg-based materials can indeed offer a new platform for fixation of a soft tissue to a bone in orthopaedic surgery. The two examples studied, namely a Mg-based interference screw for ACL reconstruction (lower extremity) and a Mg-based suture anchor for rotator cuff repair (upper extremity) clearly illustrated the potential of these devices. To recapitulate, through the use of finite element analysis, the design of a Mg-based interference screw could be optimized to make it perform at the same level of a titanium-based interference screw (Weiler et al., 1998; Zhang et al., 2007). With good fixation of the graft, ACL reconstruction with a Mg-based interference screw could restore initial knee joint stability and load the graft to the level of an intact ACL. In the follow-up in vivo study, it was demonstrated that a Mg-based alloy is biocompatible as it does not elicit adverse immune responses or toxic effects to hinder the healing of the replacement graft. These observations are in agreement with the literature on *in vivo* studies of Mg-based alloys (Windhagen et al., 2013; Witte et al., 2005). In terms of biomechanical performance after 12 weeks of healing, joint stability and graft function were lower compared to those at time zero. However, the values were comparable to the previous results of ACL reconstruction using goats (Abramowitch et al., 2003). On the other hand, the stiffness of the femur-graft-tibia complex at 12 weeks was comparable to that at time zero, indicating fixation remained intact and the graft healed properly. We did not observe statistically significant difference in the ultimate load between the two time point either,

while there was a significant reduction in the ultimate elongation. These values were comparable to those from past studies of ACL reconstruction in a goat model (Ng et al., 1995). Using a similar design process and methods of evaluation, Mg-based suture anchors were also successfully developed. Finite element analysis had identified the optimal design parameters for Mg-based suture anchors so that they could provide superior initial fixation over those by polymer-based suture anchors.

7.1 SPECIFIC AIM 1: DEVELOPMENT OF MG-BASED INTERFERENCE SCREW FOR ACL RECONSTRUCTION

In Specific Aim 1, a Mg-based interference screw for ACL reconstruction was developed. Along the way, we tested three hypotheses. First, we showed that the design of a Mg-based interference screw can be optimized and it can achieve comparable initial fixation compared to a titanium-based control (hypothesis 1.1). Second, ACL reconstruction using the Mg-based interference screws could restore initial knee joint stability to the same level of the intact joint and load the graft to the same level as the intact ACL (hypothesis 1.2). Finally, at 12 weeks of healing, good graft healing was confirmed as joint stability and graft function as well as the structural properties of the femur-graft-tibia complex were comparable to those from past studies of ACL reconstruction in a goat model (hypothesis 1.3).

7.1.1 Hypothesis 1.1: Initial Fixation of the ACL Replacement Graft Using a Mg-Based Interference Screw

The first hypothesis in Specific Aim 1 was that a Mg-based interference screw of similar dimensions as a titanium interference screw would achieve comparable initial fixation. Through preliminary in vitro testing, we identified that the design of the screw drive of a Mg-based

interference screw needed to be optimized as screw stripping was occurring during insertion. Using finite element analysis, it was identified that stress concentrations arose at the edges of the hexagonal drive used in the initial design, and the maximum stress in the screw was above tensile strength of pure magnesium. This guided the decision to use an alloy AZ31. Also, it was shown that the maximum von Mises stress in the screw could be reduced significantly by increasing the drive depth. Also, a square drive was chosen instead of a hexagonal drive because finite element analysis showed this change would not increase stress at the edges of the drive while it has a sharper angle at each edge to resist stripping.

The results of the cyclic loading test confirmed our hypothesis that Mg-based interference screws of similar dimensions can provide comparable initial fixation as commercially available titanium-based interference screws. After the three cyclic loading tests, the FGTCs with Mg-based interference screws had a comparable value of residual elongation as that with titanium-based interference screws. Structural properties (stiffness, ultimate load, and ultimate elongation) of the FGTCs were also comparable between the two groups, corroborating the results of the cyclic loading tests. These values were comparable to previous results obtained with ACL reconstruction in a goat model using a similar surgical procedure, where fixation was done with a titanium interference screw (Musahl et al., 2003).

These findings demonstrated feasibility of Mg-based interference screws for ACL reconstruction in terms of initial fixation. The important caveat is that the design of future Mg-based fixation devices will need to be optimized through finite element analysis and *in vitro* testing in order to achieve comparable fixation as a titanium counterpart.

7.1.2 Hypothesis 1.2: Joint Stability and Graft Function at Time Zero after ACL Reconstruction Using Mg-Based Interference Screws

We were able to confirm that ACL reconstruction with Mg-based interference screws could restore knee joint stability to the level of the intact joint and load the graft to the same level as the intact ACL. The APTT of the reconstructed joint was within 1 mm of that of the intact joint at all flexion angles, and it was a significant reduction (up to 60%) from that in the ACL-deficient joint. The in-situ force in the graft after ACL reconstruction with Mg-based interference screws was within 5 N of that in the intact ACL at all flexion angles, indicating that the fixed graft was contributing to the joint stability and the ACL function was restored. A previous study from our research center (Abramowitch et al., 2003) showed similar results at time zero in terms of the APTT and the in situ load in the graft.

These findings clearly showed that Mg-based interference screws could be used for ACL reconstruction as an alternative to the existing devices. This lend confidence to the use of Mg-based interference screws for future use in human applications. With this positive finding, the next step was to see if a Mg-based interference screw is biocompatible and could provide continued fixation to allow the graft to heal properly *in vivo*.

7.1.3 Hypothesis 1.3: In Vivo Biocompatibility and Biomechanical Performance of Mg-Based Interference Screws

From post-operative monitoring, absence of adverse effects, both local and systemic, indicate good biocompatibility of Mg-based interference screws. In terms of joint function, the APTT of the healing joint at 12 weeks was significantly higher than that of the reconstructed joint at time zero at all three angles. However, these values were comparable to previous studies using a similar animal model for ACL reconstruction (Abramowitch et al., 2003; Papageorgiou et al.,

2001). This increase in the laxity of the joint was expected as the ACL graft was undergoing a remodeling process. The in-situ force in the replacement graft at 12 weeks was also reduced compared to that at time zero at all three flexion angles. These values were also comparable to previous studies (Abramowitch et al., 2003; Papageorgiou et al., 2001).

In terms of the structural properties of the femur-graft-tibia complex at 12 weeks, we did not detect significant differences compared to those at time zero, except for the ultimate elongation. The values were also comparable to those from a past study on ACL reconstruction in a goat model (Ng et al., 1995).

Although we were not able to have a positive control where ACL reconstruction was performed with titanium-based interference screws, comparison to the results from past studies in the literature on ACL reconstruction in a goat model showed that ACL reconstruction with Mg-based interference screws performed comparably in terms of biomechanical performance. This was the case in other animal models with quantitative measures of joint function and structural properties (Ballock et al., 1989; Weiler et al., 2002), This trend found in animal models, however, does not agree with the good clinical outcomes from human patients. This discrepancy may be due to the lack of quantitative methods to evaluate the graft function and structural properties in the clinical arena. There currently does not exist conclusive evidence that the ACL replacement graft can fully replace the intact ACL even at a long term.

7.2 SPECIFIC AIM 2: DEVELOPMENT OF MG-BASED SUTURE ANCHOR FOR ROTATOR CUFF REPAIR

In Specific Aim 2, Mg-based suture anchors were developed. For this, two hypotheses were tested. First, we confirmed that the thread design of a Mg-based suture anchor can be optimized

to improve its fixation through finite element analysis (hypothesis 2.2). Second, we showed that Mg-based suture anchors can provide superior fixation over that by polymer suture anchors through tensile testing.

7.2.1 Hypothesis 2.1: Finite Element Analysis and Parametric Analysis of the Design of a Mg-Based Suture Anchor

The results of the finite element analysis and parametric analysis showed that the design of a Mg-based suture anchor could be optimized by modifying the key design parameters, thread depth and pitch, confirming our hypothesis. Increasing the thread depth and decreasing the thread pitch both could reduce von Mises stress in the Mg-based suture anchor. These findings were in agreement with previous studies looking at design of screw devices and its effect on pull-out strength (Chapman et al., 1996).

The current findings showed that a Mg-based suture anchor has a definite advantage over a polymer suture anchor as its thread can be deeper thanks to superior mechanical properties. It is often not possible to design the thread of a polymer suture anchor deep. Instead, they tend to have a small thread pitch (more threads) to increase its fixation strength (see **Figure E.1**). Hence, a Mg-based suture anchor is a superior alternative as it is biodegradable while the design can follow that of a traditional metallic suture anchor. It would make implantation easier and faster, while providing secure fixation.

Figure E.1. A: A polymer suture anchor with shallow threads with a higher number of turns. B: A titanium-based suture anchor with deeper threads and a lower number of turns. (Source: Barber et al, 2008)

7.2.2 Hypothesis 2.2: Tensile Test of Mg-Based Suture Anchors at Time Zero

With the optimized design, Mg-based suture anchors could achieve superior fixation compared to polymer suture anchors of similar dimensions as both the stiffness and ultimate load were higher for Mg-based suture anchors over polymer suture anchors. Further, the fact that Mg-based suture anchors only failed through pull-out rather than failure at the anchor itself indicates that they could resist much higher loads. In fact, we performed preliminary tensile testing of a Mg-based suture anchor in a cortical bone, and the ultimate load could reach up to more than 1000 N. These results were superior to those of commercially-available polymer suture anchors of similar dimensions in the literature (Barber and Herbert, 2013).

These positive findings indicate that Mg-based suture anchors are a superior alternative to polymer suture anchors. The superior fixation provided by Mg-based suture anchors are particularly advantageous as new and improved sutures and suturing techniques are becoming available. In the past, the common failure mechanism of rotator cuff repairs using suture anchors was the suture pulling out of the tendon substance (Cummins and Murrell, 2003). New suturing techniques with stronger sutures (Park et al., 2014) allow for a stronger tendon-suture connection,

putting higher mechanical demand on suture anchors. Hence, suture anchors that provide superior fixation would become indispensible.

7.3 LIMITATIONS AND FUTURE STUDIES

There are a few limitations to research presented in the current dissertation. First, the time point used for in vivo evaluation of the Mg-based interference screw was only for the remodeling period (12 weeks) in the goat model. Hence, the shorter and longer results of Mg-based materials on the healing process and biomechanical performance still need to be studied. Still, we performed 2 preliminary *in vivo* studies before coming to the final study to achieve successful results. As we have developed the Mg-based interference screw from scratch, the findings represent a significant milestone in proof of concept.

Second, *in vivo* evaluation was mostly limited to biomechanical performance, i.e. there was no detailed analysis of degradation and biocompatibility. As we have proved good fixation of the graft and restoration of joint function. Once these were confirmed, the future studies could use this model to address questions related to biocompatibility and device degradation. For this, more detailed evaluations of biocompatibility and degradation using histology and computed tomography need to be performed. Systemic biocompatibility should also be assessed using blood sampling and histology of kidney, liver, and so on.

Third, in terms of methods of evaluation, the loading conditions used with the robotic/UFS testing system were to simulate a clinical examination to test the ACL function. It was not to test the graft function in respect to the higher loading experienced *in vivo*. Hence, the current results only show the response of the joint and the graft in an ideal condition. Applying *in vivo* loading conditions could better test the joint kinematics and graft function after ACL

reconstruction with Mg-based interference screws. This will entail obtaining *in vivo* kinematics from live animals or human subjects using a biplane fluoroscope and replaying on cadaver joints to find out how the joint and its components are loaded under *in vivo* conditions (Woo et al., 2006). This information could be used to assess the outcome of ACL reconstruction with Mg-based interference screws under realistic loading conditions.

Fourth, the results may not translate directly to human applications although it was done with a large animal study. Particularly, the human immune system is quite different from that of a goat. The goat model was the best model that was available to perform a proof-of-concept *in vivo* study as we have extensive experience studying ACL reconstruction in this model with good results. Eventually, clinical trials with human subjects are required to study biocompatibility of Mg-based materials and human inflammatory responses. This will require more thorough evaluation in the animal model as outlined above. Also, novel alloys produced with medical grade materials and manufacturing processes will be needed. Hence, further developments in these areas are absolutely required.

Another limitation associated with the animal model was that rehabilitation could not be controlled. This may have had some influence on the results, as rehabilitation protocols have shown to affect the healing of the graft after ACL reconstruction (Shelbourne et al., 1991). Most past animal studies of ACL reconstruction with quantitative assessment showed poor outcome in terms of joint stability and structural properties, while the subjective clinical outcomes of ACL reconstruction have been overall good. Hence, novel methods to lessen the excessive loading on the graft and allow careful rehabilitation of animals immediately after surgery could lead to improved results (Gelberman et al., 1982; Woo et al., 1981).

Fifth, the computational model was limited to simplified geometry, loading conditions, and boundary conditions. It was based on an ideal testing condition of a load-to-failure test in a polyurethane foam. Also, we limited our analysis to mechanical analysis although one of the key aspect of Mg-based interference screws is that they will degrade. Degradation and mechanical behavior will affect each other significantly. Building on the current finite element model, one could use more realistic geometries and material properties to simulate an actual bone to see how the design of a Mg-based fixation device could be optimized further. Further, degradation of the Mg-based alloy can be incorporated to see how mechanical loads impact degradation and how degradation impacts mechanical performance over time.

Finally, the material (AZ31) used for the current study was a commercially available alloy for industrial use, which makes it unsuitable for medical devices for both regulatory and business-related reasons. The rationale to choose a commercially available alloy AZ31 was that it has good corrosion resistance with consistent mechanical properties. With this alloy, degradation would be minimal at 12 weeks so that fixation is not lost. Also, good mechanical properties allowed for proper implantation without mechanical failure. However, further developments with different alloys and surface treatments should be explored to even further improve biocompatibility and fine-tune degradation rates. New alloys will have to be developed to make it more desirable for clinical application in terms of regulatory and commercialization purposes.

8.0 CONCLUSIONS

8.1 ENGINEERING SIGNIFICANCE

The current dissertation established a complete set of tools to design and evaluate Mg-based fixation devices for orthopaedic surgery. Using the computational approaches, it was possible to evaluate and optimize the design of the devices before extensive *in vivo* tests in a costly animal model. This approach will be very effective for development of other devices by saving time and money to perform unnecessary animal studies. Quantitative biomechanical tests using the robotic/UFS testing system and a material testing machine allowed for objective and accurate assessment of biomechanical performance of these devices at multiple time points in a realistic surgical model. The methods established here could be used for further development of Mg-based interference screws or suture anchors, as well as other devices.

8.2 SCIENTIFIC SIGNIFICANCE

The current dissertation established an appropriate and realistic large animal model to evaluate biodegradable metallic implants for soft tissue fixation in orthopaedics. Current study was performed under a realistic loading condition where micromotion of the tissue around the implant could have affected healing, adding relevant data to the existing literature where only

simple implantation without mechanical loading was studied. Thus, using this model, further studies on magnesium degradation and its impact on bone/ligament healing can be performed.

8.3 CLINICAL SIGNIFICANCE

As current biodegradable screws and suture anchors made with polymer materials have led to complications, magnesium-based devices present a compelling alternative as they can reduce complications while enhancing the tissue healing. This would lead to improved surgical outcome as well as better patient satisfaction. In fact, currently, there are multiple groups in Europe and Asia that are performing clinical trials of Mg-based fixation devices with excellent outcomes (Windhagen, 2013).

Through the development of Mg-based interference screws for ACL reconstruction, biocompatibility of Mg-based alloys as well as in vivo outcomes in terms of joint stability and graft function have been verified. These results can be served as the basis for future studies to facilitate and accelerate translation of the technology to clinical application. The process using computational analysis and experimental verification proved to be an effective way to optimize the performance of new devices. As such, this approach can be applied to tailor design of other devices to repair Achilles tendon, lateral collateral ligament (LCL), medial patellofemoral ligament (MPFL), and so on, where similar screws or suture anchors are required for surgical reconstruction.

BIBLIOGRAPHY

AAOS, 2008. United States Bone and Joint Decade: The Burden of Musculoskeletal Diseases in the United States. American Academy of Orthopaedic Surgeons, Rosemont, IL.

Abramowitch, S.D., Papageorgiou, C.D., Withrow, J.D., Gilbert, T.W., Woo, S.L-Y., 2003. The effect of initial graft tension on the biomechanical properties of a healing ACL replacement graft: a study in goats. Journal of Orthopaedic Research 21, 708-715.

Agel, J., Olson, D.E., Dick, R., Arendt, E.A., Marshall, S.W., Sikka, R.S., 2007. Descriptive epidemiology of collegiate women's basketball injuries: National Collegiate Athletic Association Injury Surveillance System, 1988-1989 through 2003-2004. J Athl Train 42, 202-210.

Aglietti, P., Buzzi, R., Zaccherotti, G., De Biase, P., 1994. Patellar tendon versus doubled semitendinosus and gracilis tendons for anterior cruciate ligament reconstruction. Am J Sports Med 22, 211-217; discussion 217-218.

Aglietti, P., Giron, F., Buzzi, R., Biddau, F., Sasso, F., 2004. Anterior cruciate ligament reconstruction: bone-patellar tendon-bone compared with double semitendinosus and gracilis tendon grafts. A prospective, randomized clinical trial. The Journal of bone and joint surgery. American volume 86-A, 2143-2155.

Ahmad, C.S., Kwak, S.D., Ateshian, G.A., Warden, W.H., Steadman, J.R., Mow, V.C., 1998. Effects of patellar tendon adhesion to the anterior tibia on knee mechanics. Am J Sports Med 26, 715-724.

Andersson, C., Odensten, M., Good, L., Gillquist, J., 1989. Surgical or non-surgical treatment of acute rupture of the anterior cruciate ligament. A randomized study with long-term follow-up. The Journal of bone and joint surgery. American volume 71, 965-974.

Apreleva, M., Ozbaydar, M., Fitzgibbons, P.G., Warner, J.J., 2002. Rotator cuff tears: the effect of the reconstruction method on three-dimensional repair site area. Arthroscopy 18, 519-526.

Badylak, S.F., Freytes, D.O., Gilbert, T.W., 2009. Extracellular matrix as a biological scaffold material: Structure and function. Acta Biomater 5, 1-13.

Badylak, S.F., Valentin, J.E., Ravindra, A.K., McCabe, G.P., Stewart-Akers, A.M., 2008. Macrophage phenotype as a determinant of biologic scaffold remodeling. Tissue Eng Part A 14, 1835-1842.

Ballock, R.T., Woo, S.L-Y., Lyon, R.M., Hollis, J.M., Akeson, W.H., 1989. Use of patellar tendon autograft for anterior cruciate ligament reconstruction in the rabbit: a long-term histologic and biomechanical study. J Orthop Res 7, 474-485.

Barber, F.A., Boothby, M.H., 2007. Bilok interference screws for anterior cruciate ligament reconstruction: clinical and radiographic outcomes. Arthroscopy 23, 476-481.

Barber, F.A., Dockery, W.D., 2008. Long-term absorption of beta-tricalcium phosphate poly-L-lactic acid interference screws. Arthroscopy 24, 441-447.

Barber, F.A., Elrod, B.F., McGuire, D.A., Paulos, L.E., 1995. Preliminary results of an absorbable interference screw. Arthroscopy 11, 537-548.

Barber, F.A., Herbert, M.A., 2013. Cyclic Loading Biomechanical Analysis of the Pullout Strengths of Rotator Cuff and Glenoid Anchors: 2013 Update. Arthroscopy-the Journal of Arthroscopic and Related Surgery 29, 832-844.

Barber, F.A., Herbert, M.A., Beavis, R.C., Barrera Oro, F., 2008. Suture anchor materials, eyelets, and designs: update 2008. Arthroscopy 24, 859-867.

Barrett, G.R., Noojin, F.K., Hartzog, C.W., Nash, C.R., 2002. Reconstruction of the anterior cruciate ligament in females: A comparison of hamstring versus patellar tendon autograft. Arthroscopy 18, 46-54.

Baumgarten, K.M., Gerlach, D., Galatz, L.M., Teefey, S.A., Middleton, W.D., Ditsios, K., Yamaguchi, K., 2010. Cigarette smoking increases the risk for rotator cuff tears. Clin Orthop Relat Res 468, 1534-1541.

Baums, M.H., Zelle, B.A., Schultz, W., Ernstberger, T., Klinger, H.M., 2006. Intraarticular migration of a broken biodegradable interference screw after anterior cruciate ligament reconstruction. Knee surgery, sports traumatology, arthroscopy : official journal of the ESSKA 14, 865-868.

Beaty, J., 1999. Knee and leg: soft tissue trauma, in: Arendt, E.A. (Ed.), OKU orthopaedic knowledge update, 1st ed. American Academy of Orthopaedic Surgeons, Rosemont, IL, pp. xix, 442.

Beevers, D.J., 2003. Metal vs bioabsorbable interference screws: initial fixation. Proc Inst Mech Eng H 217, 59-75.

Beynnon, B.D., Johnson, R.J., Fleming, B.C., Kannus, P., Kaplan, M., Samani, J., Renstrom, P., 2002. Anterior cruciate ligament replacement: comparison of bone-patellar tendon-bone grafts with two-strand hamstring grafts. A prospective, randomized study. The Journal of bone and joint surgery. American volume 84-A, 1503-1513.

Bishop, J., Klepps, S., Lo, I.K., Bird, J., Gladstone, J.N., Flatow, E.L., 2006. Cuff integrity after arthroscopic versus open rotator cuff repair: a prospective study. J Shoulder Elbow Surg 15, 290-299.

Boffa, M.C., Boinot, C., De Carolis, S., Rovere-Querini, P., Aurousseau, M.H., Allegri, F., Nicaise-Roland, P., Barra, A., Botta, A., Ambrozic, A., Avcin, T., Tincani, A., 2009. Laboratory criteria of the obstetrical antiphospholipid syndrome. Data from a multicentric prospective European women cohort. Thrombosis and haemostasis 102, 25-28.

Boileau, P., Brassart, N., Watkinson, D.J., Carles, M., Hatzidakis, A.M., Krishnan, S.G., 2005. Arthroscopic repair of full-thickness tears of the supraspinatus: does the tendon really heal? The Journal of bone and joint surgery. American volume 87, 1229-1240.

Bostman, O., Hirvensalo, E., Makinen, J., Rokkanen, P., 1990. Foreign-body reactions to fracture fixation implants of biodegradable synthetic polymers. J Bone Joint Surg Br 72, 592-596.

Bostman, O., Paivarinta, U., Partio, E., Vasenius, J., Manninen, M., Rokkanen, P., 1992. Degradation and tissue replacement of an absorbable polyglycolide screw in the fixation of rabbit femoral osteotomies. The Journal of bone and joint surgery. American volume 74, 1021-1031.

Bottoni, C.R., Deberardino, T.M., Fester, E.W., Mitchell, D., Penrod, B.J., 2000. An intra-articular bioabsorbable interference screw mimicking an acute meniscal tear 8 months after an anterior cruciate ligament reconstruction. Arthroscopy 16, 395-398.

Bowers, M.E., Tung, G.A., Trinh, N., Leventhal, E., Crisco, J.J., Kimia, B., Fleming, B.C., 2008. Effects of ACL interference screws on articular cartilage volume and thickness measurements with 1.5 T and 3 T MRI. Osteoarthritis Cartilage 16, 572-578.

Brand, J., Jr., Weiler, A., Caborn, D.N., Brown, C.H., Jr., Johnson, D.L., 2000. Graft fixation in cruciate ligament reconstruction. Am J Sports Med 28, 761-774.

Brand, J.C., Jr., Nyland, J., Caborn, D.N., Johnson, D.L., 2005. Soft-tissue interference fixation: bioabsorbable screw versus metal screw. Arthroscopy 21, 911-916.

Breazeale, N.M., Craig, E.V., 1997. Partial-thickness rotator cuff tears. Pathogenesis and treatment. Orthop Clin North Am 28, 145-155.

Capiola, D., Re, L., 2007. Repair of patellar tendon rupture with suture anchors. Arthroscopy 23, 906 e901-904.

Castricini, R., Longo, U.G., De Benedetto, M., Panfoli, N., Pirani, P., Zini, R., Maffulli, N., Denaro, V., 2011. Platelet-rich plasma augmentation for arthroscopic rotator cuff repair: a randomized controlled trial. Am J Sports Med 39, 258-265.

Chapman, J.R., Harrington, R.M., Lee, K.M., Anderson, P.A., Tencer, A.F., Kowalski, D., 1996. Factors affecting the pullout strength of cancellous bone screws. J Biomech Eng 118, 391-398.

Chen, C.H., Chang, C.H., Wang, K.C., Su, C.I., Liu, H.T., Yu, C.M., Wong, C.B., Wang, I.C., Whu, S.W., Liu, H.W., 2011. Enhancement of rotator cuff tendon-bone healing with

injectable periosteum progenitor cells-BMP-2 hydrogel in vivo. Knee surgery, sports traumatology, arthroscopy : official journal of the ESSKA 19, 1597-1607.

Chen, C.H., Chuang, T.Y., Wang, K.C., Chen, W.J., Shih, C.H., 2006. Arthroscopic anterior cruciate ligament reconstruction with quadriceps tendon autograft: clinical outcome in 4-7 years. Knee surgery, sports traumatology, arthroscopy : official journal of the ESSKA 14, 1077-1085.

Chowdhury, P., Matyas, J.R., Frank, C.B., 1991. The "epiligament" of the rabbit medial collateral ligament: a quantitative morphological study. Connective tissue research 27, 33-50.

Cojocaru, I.M., Cojocaru, M., Musuroi, C., Botezat, M., 2003. Study of anti-cardiolipin and anti-beta2-glycoprotein I antibodies in patients with ischemic stroke. Romanian journal of internal medicine = Revue roumaine de medecine interne 41, 189-204.

Cole, D.W., Ginn, T.A., Chen, G.J., Smith, B.P., Curl, W.W., Martin, D.F., Poehling, G.G., 2005. Cost comparison of anterior cruciate ligament reconstruction: Autograft versus allograft. Arthroscopy - Journal of Arthroscopic and Related Surgery 21, 786-790.

Colvin, A.C., Egorova, N., Harrison, A.K., Moskowitz, A., Flatow, E.L., 2012. National trends in rotator cuff repair. The Journal of bone and joint surgery. American volume 94, 227-233.

Cooper, R.R., Misol, S., 1970. Tendon and Ligament Insertion . A Light and Electron Microscopic Study. Journal of Bone and Joint Surgery-American Volume A 52, 1-&.

Cotton, R.E., Rideout, D.F., 1964. Tears of the Humeral Rotator Cuff; a Radiological and Pathological Necropsy Survey. J Bone Joint Surg Br 46, 314-328.

Cummins, C.A., Murrell, G.A., 2003. Mode of failure for rotator cuff repair with suture anchors identified at revision surgery. J Shoulder Elbow Surg 12, 128-133.

Daniel, D.M., Stone, M.L., Dobson, B.E., Fithian, D.C., Rossman, D.J., Kaufman, K.R., 1994. Fate of the ACL-injured patient. A prospective outcome study. Am J Sports Med 22, 632-644.

DeAngelis, J.P., Fulkerson, J.P., 2007. Quadriceps tendon--a reliable alternative for reconstruction of the anterior cruciate ligament. Clinics in sports medicine 26, 587-596.

Debski, R.E., Sakone, M., Woo, S.L-Y., Wong, E.K., Fu, F.H., Warner, J.J., 1999. Contribution of the passive properties of the rotator cuff to glenohumeral stability during anterior-posterior loading. J Shoulder Elbow Surg 8, 324-329.

Drogset, J.O., Grontvedt, T., Robak, O.R., Molster, A., Viset, A.T., Engebretsen, L., 2006. A sixteen-year follow-up of three operative techniques for the treatment of acute ruptures of the anterior cruciate ligament. The Journal of bone and joint surgery. American volume 88, 944-952.

Ernstberger, T., Buchhorn, G., Heidrich, G., 2010. Magnetic resonance imaging evaluation of intervertebral test spacers: an experimental comparison of magnesium versus titanium and carbon fiber reinforced polymers as biomaterials. Ir J Med Sci 179, 107-111.

Fealy, S., Rodeo, S.A., MacGillivray, J.D., Nixon, A.J., Adler, R.S., Warren, R.F., 2006. Biomechanical evaluation of the relation between number of suture anchors and strength of the bone-tendon interface in a goat rotator cuff model. Arthroscopy-the Journal of Arthroscopic and Related Surgery 22, 595-602.

Feller, J.A., Webster, K.E., 2003. A randomized comparison of patellar tendon and hamstring tendon anterior cruciate ligament reconstruction. Am J Sports Med 31, 564-573.

Figgie, H.E., Bahniuk, E.H., Heiple, K.G., Davy, D.T., 1986. The Effects of Tibial Femoral Angle on the Failure Mechanics of the Canine Anterior Cruciate Ligament. J Biomech 19, 89-91.

Fink, C., Benedetto, K.P., Hackl, W., Hoser, C., Freund, M.C., Rieger, M., 2000. Bioabsorbable polyglyconate interference screw fixation in anterior cruciate ligament reconstruction: a prospective computed tomography-controlled study. Arthroscopy 16, 491-498.

Fleming, B.C., Spindler, K.P., Palmer, M.P., Magarian, E.M., Murray, M.M., 2009. Collagen-Platelet Composites Improve the Biomechanical Properties of Healing Anterior Cruciate Ligament Grafts in a Porcine Model. Am J Sport Med 37, 1554-1563.

Fox, R.J., Harner, C.D., Sakane, M., Carlin, G.J., Woo, S.L-Y., 1998. Determination of the in situ forces in the human posterior cruciate ligament using robotic technology. A cadaveric study. Am J Sports Med 26, 395-401.

Franceschi, F., Ruzzini, L., Longo, U.G., Martina, F.M., Zobel, B.B., Maffulli, N., Denaro, V., 2007. Equivalent clinical results of arthroscopic single-row and double-row suture anchor repair for rotator cuff tears - A randomized controlled trial. Am J Sport Med 35, 1254-1260.

Fujie, H., Livesay, G.A., Woo, S.L-Y., Kashiwaguchi, S., Blomstrom, G., 1995. The use of a universal force-moment sensor to determine in-situ forces in ligaments: a new methodology. J Biomech Eng 117, 1-7.

Fukuda, H., 2000. Partial-thickness rotator cuff tears: a modern view on Codman's classic. J Shoulder Elbow Surg 9, 163-168.

Fukuda, H., Hamada, K., Nakajima, T., Tomonaga, A., 1994. Pathology and pathogenesis of the intratendinous tearing of the rotator cuff viewed from en bloc histologic sections. Clin Orthop Relat Res, 60-67.

Gabriel, M.T., Wong, E.K., Woo, S.L-Y., Yagi, M., Debski, R.E., 2004. Distribution of in situ forces in the anterior cruciate ligament in response to rotatory loads. J Orthop Res 22, 85-89.

Garbern, J.C., Minami, E., Stayton, P.S., Murry, C.E., 2011. Delivery of basic fibroblast growth factor with a pH-responsive, injectable hydrogel to improve angiogenesis in infarcted myocardium. Biomaterials 32, 2407-2416.

Gay, S., Arostegui, S., Lemaitre, J., 2009. Preparation and characterization of dense nanohydroxyapatite/PLLA composites. Materials Science & Engineering C-Biomimetic and Supramolecular Systems 29, 172-177.

Geib, T.M., Shelton, W.R., Phelps, R.A., Clark, L., 2009. Anterior cruciate ligament reconstruction using quadriceps tendon autograft: intermediate-term outcome. Arthroscopy 25, 1408-1414.

Gelberman, R.H., Woo, S.L-Y., Lothringer, K., Akeson, W.H., Amiel, D., 1982. Effects of early intermittent passive mobilization on healing canine flexor tendons. The Journal of hand surgery 7, 170-175.

Gleyze, P., Thomazeau, H., Flurin, P.H., Lafosse, L., Gazielly, D.F., Allard, M., 2000. [Arthroscopic rotator cuff repair: a multicentric retrospective study of 87 cases with anatomical assessment]. Revue de chirurgie orthopedique et reparatrice de l'appareil moteur 86, 566-574.

Gulotta, L.V., Kovacevic, D., Ehteshami, J.R., Dagher, E., Packer, J.D., Rodeo, S.A., 2009. Application of bone marrow-derived mesenchymal stem cells in a rotator cuff repair model. Am J Sports Med 37, 2126-2133.

Hefti, F.L., Kress, A., Fasel, J., Morscher, E.W., 1991. Healing of the transected anterior cruciate ligament in the rabbit. The Journal of bone and joint surgery. American volume 73, 373-383.

Ho, W.F., Wu, S.C., Chang, H.H., Hsu, H.C., 2010. Structure and mechanical properties of Ti-5Cr based alloy with Mo addition. Materials Science & Engineering C-Materials for Biological Applications 30, 904-909.

Hoher, J., Livesay, G.A., Ma, C.B., Withrow, J.D., Fu, F.H., Woo, S.L-Y., 1999. Hamstring graft motion in the femoral bone tunnel when using titanium button/polyester tape fixation. Knee surgery, sports traumatology, arthroscopy : official journal of the ESSKA 7, 215-219.

Hollis, J.M., Takai, S., Adams, D.J., Horibe, S., Woo, S.L-Y., 1991. The effects of knee motion and external loading on the length of the anterior cruciate ligament (ACL): a kinematic study. J Biomech Eng 113, 208-214.

Hort, N., Huang, Y., Fechner, D., Stormer, M., Blawert, C., Witte, F., Vogt, C., Drucker, H., Willumeit, R., Kainer, K.U., Feyerabend, F., 2010. Magnesium alloys as implant materials--principles of property design for Mg-RE alloys. Acta Biomater 6, 1714-1725.

Hunt, J.A., Callaghan, J.T., 2008. Polymer-hydroxyapatite composite versus polymer interference screws in anterior cruciate ligament reconstruction in a large animal model. Knee surgery, sports traumatology, arthroscopy : official journal of the ESSKA 16, 655-660.

Inoue, H., Sugahara, K., Yamamoto, A., Tsubakino, H., 2002. Corrosion rate of magnesium and its alloys in buffered chloride solutions. Corros Sci 44, 603-610.

Inoue, M., McGurk-Burleson, E., Hollis, J.M., Woo, S.L-Y., 1987. Treatment of the medial collateral ligament injury. I: The importance of anterior cruciate ligament on the varus-valgus knee laxity. Am J Sports Med 15, 15-21.

Ishizaki, T., Shigematsu, I., Saito, N., 2009. Anticorrosive magnesium phosphate coating on AZ31 magnesium alloy. Surf Coat Tech 203, 2288-2291.

Jarvela, T., Kannus, P., Jarvinen, M., 2000. Anterior knee pain 7 years after an anterior cruciate ligament reconstruction with a bone-patellar tendon-bone autograft. Scandinavian journal of medicine & science in sports 10, 221-227.

Jomha, N.M., Borton, D.C., Clingeleffer, A.J., Pinczewski, L.A., 1999. Long-term osteoarthritic changes in anterior cruciate ligament reconstructed knees. Clin Orthop Relat Res, 188-193.

Kannus, P., Jarvinen, M., 1987. Conservatively treated tears of the anterior cruciate ligament. Long-term results. The Journal of bone and joint surgery. American volume 69, 1007-1012.

Kaplan, N., Wickiewicz, T.L., Warren, R.F., 1990. Primary surgical treatment of anterior cruciate ligament ruptures. A long-term follow-up study. Am J Sports Med 18, 354-358.

Kartus, J., Movin, T., Karlsson, J., 2001. Donor-site morbidity and anterior knee problems after anterior cruciate ligament reconstruction using autografts. Arthroscopy 17, 971-980.

Keane, T.J., Londono, R., Turner, N.J., Badylak, S.F., 2012. Consequences of ineffective decellularization of biologic scaffolds on the host response. Biomaterials 33, 1771-1781.

Kumahashi, N., Kuwata, S., Tadenuma, T., Kadowaki, M., Uchio, Y., 2012. A "sandwich" method of reconstruction of the medial patellofemoral ligament using a titanium interference screw for patellar instability in skeletally immature patients. Arch Orthop Traum Su 132, 1077-1083.

Kunjukunju, S., Roy, A., Ramanathan, M., Lee, B., Candiello, J.E., Kumta, P.N., 2013. A layer-by-layer approach to natural polymer-derived bioactive coatings on magnesium alloys. Acta Biomaterialia.

Kurosaka, M., Yoshiya, S., Andrish, J.T., 1987. A biomechanical comparison of different surgical techniques of graft fixation in anterior cruciate ligament reconstruction. Am J Sports Med 15, 225-229.

Kwak, J.H., Sim, J.A., Kim, S.H., Lee, K.C., Lee, B.K., 2008. Delayed intra-articular inflammatory reaction due to poly-L-lactide bioabsorbable interference screw used in anterior cruciate ligament reconstruction. Arthroscopy 24, 243-246.

Lambert, K.L., 1983. Vascularized patellar tendon graft with rigid internal fixation for anterior cruciate ligament insufficiency. Clin Orthop Relat Res, 85-89.

Larsen, N.P., Forwood, M.R., Parker, A.W., 1987. Immobilization and retraining of cruciate ligaments in the rat. Acta orthopaedica Scandinavica 58, 260-264.

Laxdal, G., Kartus, J., Eriksson, B.I., Faxen, E., Sernert, N., Karlsson, J., 2006. Biodegradable and metallic interference screws in anterior cruciate ligament reconstruction surgery using hamstring tendon grafts: prospective randomized study of radiographic results and clinical outcome. Am J Sports Med 34, 1574-1580.

LeGeros, R.Z., 2002. Properties of osteoconductive biomaterials: calcium phosphates. Clin Orthop Relat Res, 81-98.

Lembeck, B., Wulker, N., 2005. Severe cartilage damage by broken poly-L-lactic acid (PLLA) interference screw after ACL reconstruction. Knee surgery, sports traumatology, arthroscopy : official journal of the ESSKA 13, 283-286.

Li, J., Zhou, L., Li, Z.C., 2010. Microstructures and mechanical properties of a new titanium alloy for surgical implant application. International Journal of Minerals Metallurgy and Materials 17, 185-191.

Li, J.C., He, Y., Inoue, Y., 2003. Thermal and mechanical properties of biodegradable blends of poly(L-lactic acid) and lignin. Polymer International 52, 949-955.

Liao, Y., Chen, D.S., Niu, J.L., Zhang, J., Wang, Y.P., Zhu, Z.J., Yuan, G.Y., He, Y.H., Jiang, Y., 2013. In vitro degradation and mechanical properties of polyporous CaHPO4-coated Mg-Nd-Zn-Zr alloy as potential tissue engineering scaffold. Mater. Lett. 100, 306-308.

Linsenmayer, T.F., Gibney, E., Igoe, F., Gordon, M.K., Fitch, J.M., Fessler, L.I., Birk, D.E., 1993. Type-V Collagen - Molecular-Structure and Fibrillar Organization of the Chicken Alpha-1(V) Nh2-Terminal Domain, a Putative Regulator of Corneal Fibrillogenesis. J Cell Biol 121, 1181-1189.

Lippitt, S.B., Vanderhooft, J.E., Harris, S.L., Sidles, J.A., Harryman, D.T., 2nd, Matsen, F.A., 3rd, 1993. Glenohumeral stability from concavity-compression: A quantitative analysis. J Shoulder Elbow Surg 2, 27-35.

Livesay, G.A., Fujie, H., Kashiwaguchi, S., Morrow, D.A., Fu, F.H., Woo, S.L-Y., 1995. Determination of the in situ forces and force distribution within the human anterior cruciate ligament. Ann Biomed Eng 23, 467-474.

Longo, U.G., Franceschi, F., Ruzzini, L., Rabitti, C., Morini, S., Maffulli, N., Denaro, V., 2008. Histoplathology of the supraspinatus tendon in rotator cuff tears. Am J Sport Med 36, 533-538.

Lu, Y., Markel, M.D., Nemke, B., Lee, J.S., Graf, B.K., Murphy, W.L., 2009. Influence of hydroxyapatite-coated and growth factor-releasing interference screws on tendon-bone healing in an ovine model. Arthroscopy 25, 1427-1434 e1421.

Lyon, R.M., Woo, S.L-Y., Hollis, J.M., Marcin, J.P., Lee, E.B., 1989. A New Device to Measure the Structural-Properties of the Femur-Anterior Cruciate Ligament-Tibia Complex. J Biomech Eng-T Asme 111, 350-354.

Ma, C.B., Comerford, L., Wilson, J., Puttlitz, C.M., 2006. Biomechanical evaluation of arthroscopic rotator cuff repairs: Double-row compared with single-row fixation. Journal of Bone and Joint Surgery-American Volume 88A, 403-410.

Macarini, L., Milillo, P., Mocci, A., Vinci, R., Ettorre, G.C., 2008. Poly-L-lactic acid - hydroxyapatite (PLLA-HA) bioabsorbable interference screws for tibial graft fixation in anterior cruciate ligament (ACL) reconstruction surgery: MR evaluation of osteointegration and degradation features. Radiol Med 113, 1185-1197.

Macdonald, P., Arneja, S., 2003. Biodegradable screw presents as a loose intra-articular body after anterior cruciate ligament reconstruction. Arthroscopy 19, E22-24.

Malcarney, H.L., Bonar, F., Murrell, G.A., 2005. Early inflammatory reaction after rotator cuff repair with a porcine small intestine submucosal implant: a report of 4 cases. Am J Sports Med 33, 907-911.

Mantovani, F., Trinchieri, A., Castelnuovo, C., Romano, A.L., Pisani, E., 2003. Reconstructive urethroplasty using porcine acellular matrix. Eur Urol 44, 600-602.

Meier, S.W., Meier, J.D., 2006a. The effect of double-row fixation on initial repair strength in rotator cuff repair: a biomechanical study. Arthroscopy 22, 1168-1173.

Meier, S.W., Meier, J.D., 2006b. Rotator cuff repair: the effect of double-row fixation on three-dimensional repair site. J Shoulder Elbow Surg 15, 691-696.

Mesfar, W., Shirazi-Adl, A., 2006. Biomechanics of changes in ACL and PCL material properties or prestrains in flexion under muscle force-implications in ligament reconstruction. Computer methods in biomechanics and biomedical engineering 9, 201-209.

Miyasaka, K.C., Daniel, D.M., Stone, M.L., et al., 1991. The incidence of knee ligament injuries in the general population. Am J Knee Surg 4, 3-8.

Moisala, A.S., Jarvela, T., Paakkala, A., Paakkala, T., Kannus, P., Jarvinen, M., 2008. Comparison of the bioabsorbable and metal screw fixation after ACL reconstruction with a hamstring autograft in MRI and clinical outcome: a prospective randomized study. Knee surgery, sports traumatology, arthroscopy : official journal of the ESSKA 16, 1080-1086.

Murray, M.M., Martin, S.D., Martin, T.L., Spector, M., 2000. Histological changes in the human anterior cruciate ligament after rupture. The Journal of bone and joint surgery. American volume 82-A, 1387-1397.

Musahl, V., Abramowitch, S.D., Gabriel, M.T., Debski, R.E., Hertel, P., Fu, F.H., Woo, S.L-Y., 2003. Tensile properties of an anterior cruciate ligament graft after bone-patellar tendon-bone

press-fit fixation. Knee surgery, sports traumatology, arthroscopy : official journal of the ESSKA 11, 68-74.

Myer, G.D., Ford, K.R., Khoury, J., Succop, P., Hewett, T.E., 2011. Biomechanics laboratory-based prediction algorithm to identify female athletes with high knee loads that increase risk of ACL injury. British journal of sports medicine 45, 245-252.

Myers, C.A., Torry, M.R., Peterson, D.S., Shelburne, K.B., Giphart, J.E., Krong, J.P., Woo, S.L-Y., Steadman, J.R., 2011. Measurements of tibiofemoral kinematics during soft and stiff drop landings using biplane fluoroscopy. Am J Sports Med 39, 1714-1722.

Nakamura, N., Horibe, S., Sasaki, S., Kitaguchi, T., Tagami, M., Mitsuoka, T., Toritsuka, Y., Hamada, M., Shino, K., 2002. Evaluation of active knee flexion and hamstring strength after anterior cruciate ligament reconstruction using hamstring tendons. Arthroscopy 18, 598-602.

Neri, B.R., Chan, K.W., Kwon, Y.W., 2009. Management of massive and irreparable rotator cuff tears. J Shoulder Elbow Surg 18, 808-818.

Ng, G.Y., Oakes, B.W., Deacon, O.W., McLean, I.D., Lampard, D., 1995. Biomechanics of patellar tendon autograft for reconstruction of the anterior cruciate ligament in the goat: three-year study. J Orthop Res 13, 602-608.

Niyibizi, C., Visconti, C.S., Kavalkovich, K., Woo, S.L-Y., 1995. Collagens in an adult bovine medial collateral ligament: Immunofluorescence localization by confocal microscopy reveals that type XIV collagen predominates at the ligament-bone junction. Matrix Biol 14, 743-751.

Noyes, F.R., Butler, D.L., Grood, E.S., Zernicke, R.F., Hefzy, M.S., 1984. Biomechanical analysis of human ligament grafts used in knee-ligament repairs and reconstructions. The Journal of bone and joint surgery. American volume 66, 344-352.

Noyes, F.R., Matthews, D.S., Mooar, P.A., Grood, E.S., 1983. The symptomatic anterior cruciate-deficient knee. Part II: the results of rehabilitation, activity modification, and counseling on functional disability. The Journal of bone and joint surgery. American volume 65, 163-174.

Ozbaydar, M., Elhassan, B., Warner, J.J.P., 2007. The use of anchors in shoulder surgery: A shift from metallic to bioabsorbable anchors. Arthroscopy-the Journal of Arthroscopic and Related Surgery 23, 1124-1126.

Padua, D.A., Marshall, S.W., Boling, M.C., Thigpen, C.A., Garrett, W.E., Jr., Beutler, A.I., 2009. The Landing Error Scoring System (LESS) Is a valid and reliable clinical assessment tool of jump-landing biomechanics: The JUMP-ACL study. Am J Sports Med 37, 1996-2002.

Papageorgiou, C.D., Ma, C.B., Abramowitch, S.D., Clineff, T.D., Woo, S.L-Y., 2001. A multidisciplinary study of the healing of an intraarticular anterior cruciate ligament graft in a goat model. Am J Sports Med 29, 620-626.

Paramsothy, M., Hassan, S.F., Srikanth, N., Gupta, M., 2010. Simultaneous enhancement of tensile/compressive strength and ductility of magnesium alloy AZ31 using carbon nanotubes. J Nanosci Nanotechnol 10, 956-964.

Park, M.C., Peterson, A., Patton, J., McGarry, M.H., Park, C.J., Lee, T.Q., 2014. Biomechanical effects of a 2 suture-pass medial inter-implant mattress on transosseous-equivalent rotator cuff repair and considerations for a "technical efficiency ratio". J Shoulder Elbow Surg 23, 361-368.

Pattee, G.A., Fox, J.M., Del Pizzo, W., Friedman, M.J., 1989. Four to ten year followup of unreconstructed anterior cruciate ligament tears. Am J Sports Med 17, 430-435.

Philippon, M.J., Arnoczky, S.P., Torrie, A., 2007. Arthroscopic repair of the acetabular labrum: a histologic assessment of healing in an ovine model. Arthroscopy 23, 376-380.

Rudy, T.W., Livesay, G.A., Woo, S.L-Y., Fu, F.H., 1996. A combined robotic/universal force sensor approach to determine in situ forces of knee ligaments. J Biomech 29, 1357-1360.

Safran, M.R., Harner, C.D., 1996. Technical considerations of revision anterior cruciate ligament surgery. Clin Orthop Relat Res, 50-64.

Sakane, M., Fox, R.J., Woo, S.L-Y., Livesay, G.A., Li, G., Fu, F.H., 1997. In situ forces in the anterior cruciate ligament and its bundles in response to anterior tibial loads. J Orthop Res 15, 285-293.

Sasaki, N., Farraro, K.F., Kim, K.E., Woo, S.L-Y., 2014. Biomechanical Evaluation of the Quadriceps Tendon Autograft for Anterior Cruciate Ligament Reconstruction: A Cadaveric Study. The American Journal of Sports Medicine.

Satku, K., Kumar, V.P., Ngoi, S.S., 1986. Anterior cruciate ligament injuries. To counsel or to operate? J Bone Joint Surg Br 68, 458-461.

Schmitz, R.J., Kulas, A.S., Perrin, D.H., Riemann, B.L., Shultz, S.J., 2007. Sex differences in lower extremity biomechanics during single leg landings. Clinical biomechanics 22, 681-688.

Segawa, H., Omori, G., Tomita, S., Koga, Y., 2001. Bone tunnel enlargement after anterior cruciate ligament reconstruction using hamstring tendons. Knee surgery, sports traumatology, arthroscopy : official journal of the ESSKA 9, 206-210.

Selmi, T.A.S., Fithian, D., Neyret, P., 2006. The evolution of osteoarthritis in 103 patients with ACL reconstruction at 17 years follow-up. Knee 13, 353-358.

Shafer, B.L., Simonian, P.T., 2002. Broken poly-L-lactic acid interference screw after ligament reconstruction. Arthroscopy 18, E35.

Shelbourne, K.D., Wilckens, J.H., Mollabashy, A., DeCarlo, M., 1991. Arthrofibrosis in acute anterior cruciate ligament reconstruction. The effect of timing of reconstruction and rehabilitation. Am J Sports Med 19, 332-336.

Shellock, F.G., Mink, J.H., Curtin, S., Friedman, M.J., 1992. MR imaging and metallic implants for anterior cruciate ligament reconstruction: assessment of ferromagnetism and artifact. J Magn Reson Imaging 2, 225-228.

Shen, C., Jiang, S.D., Jiang, L.S., Dai, L.Y., 2010. Bioabsorbable versus metallic interference screw fixation in anterior cruciate ligament reconstruction: a meta-analysis of randomized controlled trials. Arthroscopy 26, 705-713.

Smith, C.A., Tennent, T.D., Pearson, S.E., Beach, W.R., 2003. Fracture of Bilok interference screws on insertion during anterior cruciate ligament reconstruction. Arthroscopy 19, E115-117.

Snyder, S.J., 1997. Technique of arthroscopic rotator cuff repair using implantable 4-mm Revo suture anchors, suture Shuttle Relays, and no. 2 nonabsorbable mattress sutures. Orthop Clin North Am 28, 267-275.

Soslowsky, L.J., Thomopoulos, S., Esmail, A., Flanagan, C.L., Iannotti, J.P., Williamson, J.D., Carpenter, J.E., 2002. Rotator cuff tendinosis in an animal model: Role of extrinsic and overuse factors. Annals of Biomedical Engineering 30, 1057-1063.

Spindler, K.P., Kuhn, J.E., Freedman, K.B., Matthews, C.E., Dittus, R.S., Harrell, F.E., Jr., 2004. Anterior cruciate ligament reconstruction autograft choice: bone-tendon-bone versus hamstring: does it really matter? A systematic review. Am J Sports Med 32, 1986-1995.

Stahelin, A.C., Weiler, A., Rufenacht, H., Hoffmann, R., Geissmann, A., Feinstein, R., 1997. Clinical degradation and biocompatibility of different bioabsorbable interference screws: a report of six cases. Arthroscopy 13, 238-244.

Staiger, M.P., Pietak, A.M., Huadmai, J., Dias, G., 2006. Magnesium and its alloys as orthopedic biomaterials: a review. Biomaterials 27, 1728-1734.

Suchenski, M., McCarthy, M.B., Chowaniec, D., Hansen, D., McKinnon, W., Apostolakos, J., Arciero, R., Mazzocca, A.D., 2010a. Material properties and composition of soft-tissue fixation. Arthroscopy 26, 821-831.

Suchenski, M., McCarthy, M.B., Chowaniec, D., Hansen, D., McKinnon, W., Apostolakos, J., Arciero, R., Mazzocca, A.D., 2010b. Material Properties and Composition of Soft-Tissue Fixation. Arthroscopy-the Journal of Arthroscopic and Related Surgery 26, 821-831.

Tanaka, M., Itoi, E., Sato, K., Hamada, J., Hitachi, S., Tojo, Y., Honda, M., Tabata, S., 2010. Factors related to successful outcome of conservative treatment for rotator cuff tears. Upsala journal of medical sciences 115, 193-200.

Tanzer, M.L., Waite, J.H., 1982. Collagen cross-linking. Collagen and related research 2, 177-180.

Tay, B.K., Patel, V.V., Bradford, D.S., 1999. Calcium sulfate- and calcium phosphate-based bone substitutes. Mimicry of the mineral phase of bone. Orthop Clin North Am 30, 615-623.

Tecklenburg, K., Burkart, P., Hoser, C., Rieger, M., Fink, C., 2006. Prospective evaluation of patellar tendon graft fixation in anterior cruciate ligament reconstruction comparing composite bioabsorbable and allograft interference screws. Arthroscopy 22, 993-999.

Tomita, F., Yasuda, K., Mikami, S., Sakai, T., Yamazaki, S., Tohyama, H., 2001. Comparisons of intraosseous graft healing between the doubled flexor tendon graft and the bone-patellar tendon-bone graft in anterior cruciate ligament reconstruction. Arthroscopy 17, 461-476.

Venter, J.C., Adams, M.D., Myers, E.W., Li, P.W., Mural, R.J., Sutton, G.G., Smith, H.O., Yandell, M., Evans, C.A., Holt, R.A., Gocayne, J.D., Amanatides, P., et al., 2001. The sequence of the human genome. Science 291, 1304-1351.

Walla, D.J., Albright, J.P., McAuley, E., Martin, R.K., Eldridge, V., El-Khoury, G., 1985. Hamstring control and the unstable anterior cruciate ligament-deficient knee. Am J Sports Med 13, 34-39.

Walton, M., Cotton, N.J., 2007. Long-term in vivo degradation of poly-L-lactide (PLLA) in bone. J Biomater Appl 21, 395-411.

Waselau, M., Samii, V.F., Weisbrode, S.E., Litsky, A.S., Bertone, A.L., 2007. Effects of a magnesium adhesive cement on bone stability and healing following a metatarsal osteotomy in horses. Am J Vet Res 68, 370-378.

Wei, J., Jia, J.F., Wu, F., Wei, S.C., Zhou, H.J., Zhang, H.B., Shin, J.W., Liu, C.S., 2010. Hierarchically microporous/macroporous scaffold of magnesium-calcium phosphate for bone tissue regeneration. Biomaterials 31, 1260-1269.

Weiler, A., Hoffmann, R.F., Sudkamp, N.P., Siepe, C.J., Haas, N.P., 1999. Replacement of the anterior cruciate ligament. Biomechanical studies for patellar and semitendinosus tendon fixation with a poly(D,L-lactide) interference screw. Unfallchirurg 102, 115-123.

Weiler, A., Peine, R., Pashmineh-Azar, A., Abel, C., Sudkamp, N.P., Hoffmann, R.F., 2002. Tendon healing in a bone tunnel. Part I: Biomechanical results after biodegradable interference fit fixation in a model of anterior cruciate ligament reconstruction in sheep. Arthroscopy 18, 113-123.

Weiler, A., Windhagen, H.J., Raschke, M.J., Laumeyer, A., Hoffmann, R.F., 1998. Biodegradable interference screw fixation exhibits pull-out force and stiffness similar to titanium screws. Am J Sports Med 26, 119-126.

Willbold, E., Kaya, A.A., Kaya, R.A., Beckmann, F., Witte, F., 2011. Corrosion of magnesium alloy AZ31 screws is dependent on the implantation site. Mater. Sci. Eng. B-Adv. Funct. Solid-State Mater. 176, 1835-1840.

Windhagen, H., Radtke, K., Weizbauer, A., Diekmann, J., Noll, Y., Kreimeyer, U., Schavan, R., Stukenborg-Colsman, C., Waizy, H., 2013. Biodegradable magnesium-based screw clinically equivalent to titanium screw in hallux valgus surgery: short term results of the first

prospective, randomized, controlled clinical pilot study. Biomedical engineering online 12, 62.

Witte, F., The history of biodegradable magnesium implants: a review. Acta Biomater 6, 1680-1692.

Witte, F., 2010. The history of biodegradable magnesium implants: A review. Acta Biomaterialia 6, 1680-1692.

Witte, F., Fischer, J., Nellesen, J., Crostack, H.A., Kaese, V., Pisch, A., Beckmann, F., Windhagen, H., 2006. In vitro and in vivo corrosion measurements of magnesium alloys. Biomaterials 27, 1013-1018.

Witte, F., Kaese, V., Haferkamp, H., Switzer, E., Meyer-Lindenberg, A., Wirth, C.J., Windhagen, H., 2005. In vivo corrosion of four magnesium alloys and the associated bone response. Biomaterials 26, 3557-3563.

Witte, F., Ulrich, H., Palm, C., Willbold, E., 2007. Biodegradable magnesium scaffolds: Part II: peri-implant bone remodeling. Journal of Biomedical Materials Research Part A 81, 757-765.

Woo, S.L-Y., Hollis, J.M., Adams, D.J., Lyon, R.M., Takai, S., 1991. Tensile properties of the human femur-anterior cruciate ligament-tibia complex. The effects of specimen age and orientation. Am J Sports Med 19, 217-225.

Woo, S.L-Y., Orlando, C.A., Camp, J.F., Akeson, W.H., 1986. Effects of postmortem storage by freezing on ligament tensile behavior. J Biomech 19, 399-404.

Woo, S.L-Y., Abramowitch, S.D., Kilger, R., Liang, R., 2006. Biomechanics of knee ligaments: injury, healing, and repair. J Biomech 39, 1-20.

Woo, S.L-Y., Danto, M.I., Ohland, K.J., Lee, T.Q., Newton, P.O., 1990. The use of a laser micrometer system to determine the cross-sectional shape and area of ligaments: a comparative study with two existing methods. J Biomech Eng 112, 426-431.

Woo, S.L-Y., Debski, R.E., Withrow, J.D., Janaushek, M.A., 1999a. Biomechanics of knee ligaments. Am J Sports Med 27, 533-543.

Woo, S.L-Y., Debski, R.E., Wong, E.K., Yagi, M., Tarinelli, D., 1999b. Use of robotic technology for diathrodial joint research. J Sci Med Sport 2, 283-297.

Woo, S.L-Y., Gelberman, R.H., Cobb, N.G., Amiel, D., Lothringer, K., Akeson, W.H., 1981. The importance of controlled passive mobilization on flexor tendon healing. A biomechanical study. Acta orthopaedica Scandinavica 52, 615-622.

Woo, S.L-Y., Gomez, M.A., Woo, Y.K., Akeson, W.H., 1982. Mechanical properties of tendons and ligaments. II. The relationships of immobilization and exercise on tissue remodeling. Biorheology 19, 397-408.

Woo, S.L-Y., Gomez, M.A., Sites, T.J., Newton, P.O., Orlando, C.A., Akeson, W.H., 1987a. The Biomechanical and Morphological-Changes in the Medial Collateral Ligament of the Rabbit after Immobilization and Remobilization. Journal of Bone and Joint Surgery-American Volume 69A, 1200-1211.

Woo, S.L-Y., Hollis, J.M., Roux, R.D., Gomez, M.A., Inoue, M., Kleiner, J.B., Akeson, W.H., 1987b. Effects of Knee Flexion on the Structural-Properties of the Rabbit Femur-Anterior Cruciate Ligament-Tibia Complex (Fatc). J Biomech 20, 557-563.

Woo, S.L-Y., Lee, T.Q., Gomez, M.A., Sato, S., Field, F.P., 1987c. Temperature-Dependent Behavior of the Canine Medial Collateral Ligament. J Biomech Eng-T Asme 109, 68-71.

Xu, L.P., Pan, F., Yu, G.N., Yang, L., Zhang, E.L., Yang, K., 2009. In vitro and in vivo evaluation of the surface bioactivity of a calcium phosphate coated magnesium alloy. Biomaterials 30, 1512-1523.

Yaremchuk, M.J., Posnick, J.C., 1995. Resolving controversies related to plate and screw fixation in the growing craniofacial skeleton. The Journal of craniofacial surgery 6, 525-538.

Yoshiya, S., Andrish, J.T., Manley, M.T., Bauer, T.W., 1987. Graft tension in anterior cruciate ligament reconstruction. An in vivo study in dogs. Am J Sports Med 15, 464-470.

Zantop, T., Weimann, A., Schmidtko, R., Herbort, M., Raschke, M.J., Petersen, W., 2006. Graft laceration and pullout strength of soft-tissue anterior cruciate ligament reconstruction: in vitro study comparing titanium, poly-d,l-lactide, and poly-d,l-lactide-tricalcium phosphate screws. Arthroscopy 22, 1204-1210.

Zberg, B., Uggowitzer, P.J., Loffler, J.F., 2009. MgZnCa glasses without clinically observable hydrogen evolution for biodegradable implants. Nat Mater 8, 887-891.

Zhang, A.L., Lewicky, Y.M., Oka, R., Mahar, A., Pedowitz, R., 2007. Biomechanical analysis of femoral tunnel pull-out angles for anterior cruciate ligament reconstruction with bioabsorbable and metal interference screws. Am J Sports Med 35, 637-642.

Zhang, E., Xu, L., Yu, G., Pan, F., Yang, K., 2009. In vivo evaluation of biodegradable magnesium alloy bone implant in the first 6 months implantation. Journal of biomedical materials research. Part A 90, 882-893.

Zheng, M.H., Chen, J., Kirilak, Y., Willers, C., Xu, J., Wood, D., 2005. Porcine small intestine submucosa (SIS) is not an acellular collagenous matrix and contains porcine DNA: possible implications in human implantation. J Biomed Mater Res B Appl Biomater 73, 61-67.